



**HAL**  
open science

## Reprogramming dysfunctional CD8+ T cells to promote properties associated with natural HIV control

Federico Perdomo-Celis, Caroline Passaes, Valérie Monceaux, Stevonn Volant, Faroudy Boufassa, Pierre de Truchis, Morgane Marcou, Katia Bourdic, Laurence Weiss, Corinne Jung, et al.

### ► To cite this version:

Federico Perdomo-Celis, Caroline Passaes, Valérie Monceaux, Stevonn Volant, Faroudy Boufassa, et al.. Reprogramming dysfunctional CD8+ T cells to promote properties associated with natural HIV control. *The Journal of clinical investigation*, 2022, 132 (11), pp.e157549. 10.1172/jci157549. hal-03679642

**HAL Id: hal-03679642**

**<https://hal.science/hal-03679642v1>**

Submitted on 26 May 2022

**HAL** is a multi-disciplinary open access archive for the deposit and dissemination of scientific research documents, whether they are published or not. The documents may come from teaching and research institutions in France or abroad, or from public or private research centers.

L'archive ouverte pluridisciplinaire **HAL**, est destinée au dépôt et à la diffusion de documents scientifiques de niveau recherche, publiés ou non, émanant des établissements d'enseignement et de recherche français ou étrangers, des laboratoires publics ou privés.



Distributed under a Creative Commons Attribution 4.0 International License

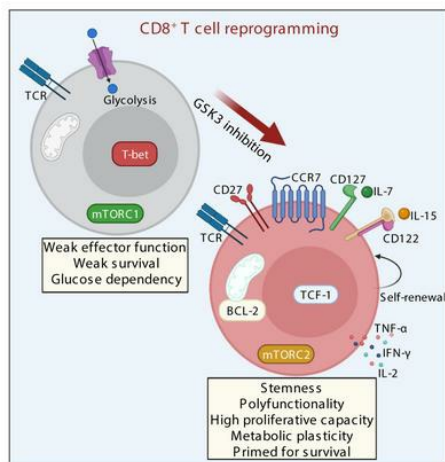
## Reprogramming dysfunctional CD8<sup>+</sup> T cells to promote properties associated with natural HIV control

Federico Perdomo-Celis, ... , Olivier Lambotte, Asier Sáez-Cirión

*J Clin Invest.* 2022. <https://doi.org/10.1172/JCI157549>.

Research In-Press Preview AIDS/HIV Immunology

### Graphical abstract



Find the latest version:

<https://jci.me/157549/pdf>



1           **Reprogramming dysfunctional CD8<sup>+</sup> T cells to promote properties**  
2   **associated with natural HIV control**

3 Federico Perdomo-Celis<sup>1</sup>, Caroline Passaes<sup>1</sup>, Valérie Monceaux<sup>1</sup>, Stevonn Volant<sup>2</sup>, Faroudy  
4 Boufassa<sup>3</sup>, Pierre de Truchis<sup>4</sup>, Morgane Marcou<sup>4</sup>, Katia Bourdic<sup>5</sup>, Laurence Weiss<sup>6</sup>, Corinne  
5 Jung<sup>6</sup>, Christine Bourgeois<sup>5</sup>, Cécile Goujard<sup>7</sup>, Laurence Meyer<sup>3</sup>, Michaela Müller-Trutwin<sup>1</sup>,  
6 Olivier Lambotte<sup>5</sup>, and Asier Sáez-Cirión<sup>1,\*</sup>

7 <sup>1</sup>Institut Pasteur, Université Paris Cité, Unité HIV Inflammation et Persistance, F-75015 Paris,  
8 France.

9 <sup>2</sup>Institut Pasteur, Université Paris Cité, Hub Bioinformatique et Biostatistique, F-75015 Paris,  
10 France.

11 <sup>3</sup>Université Paris Saclay; Inserm CESP U1018; APHP, Department of Public Health, Bicêtre  
12 Hospital, Paris Saclay, France.

13 <sup>4</sup>Université Paris-Saclay, AP-HP Hôpital Raymond Poincaré, Garches, France

14 <sup>5</sup>Université Paris-Saclay, AP-HP, Bicêtre Hospital, UMR1184 INSERM CEA, Le Kremlin  
15 Bicêtre, France.

16 <sup>6</sup>Université de Paris Cité, AP-HP, Paris Centre, Hôtel Dieu, Paris, France

17 <sup>7</sup>Université Paris-Saclay, AP-HP, Hôpital Bicêtre, DMU 7, Inserm U1018, CESP, 94290, Le  
18 Kremlin Bicêtre, France.

19 \*Corresponding author:

20 Asier Sáez-Cirión, Institut Pasteur, HIV inflammation and persistence, 25 rue du Docteur  
21 Roux, 75015 Paris, France. Tel : +33145688944. E-mail : [asier.saez-cirion@pasteur.fr](mailto:asier.saez-cirion@pasteur.fr)

22 **ABSTRACT**

23

24 Virus-specific CD8<sup>+</sup> T cells play a central role in HIV-1 natural controllers to maintain  
25 suppressed viremia in the absence of antiretroviral therapy. These cells display a memory  
26 program that confers them stemness properties, high survival, polyfunctionality, proliferative  
27 capacity, metabolic plasticity, and antiviral potential. The development and maintenance of  
28 such qualities by memory CD8<sup>+</sup> T cells appear crucial to achieving natural HIV-1 control. Here  
29 we show that targeting the signaling pathways Wnt/TCF-1 and mTORC through GSK3  
30 inhibition to reprogram HIV-specific CD8<sup>+</sup> T cells from non-controllers promoted functional  
31 capacities associated with natural control of infection. Features of such reprogrammed cells  
32 included the enrichment in TCF-1<sup>+</sup> less-differentiated subsets, superior response to antigen,  
33 enhanced survival, polyfunctionality, metabolic plasticity, less mTORC1-dependency,  
34 improved response to  $\gamma$ -chain cytokines and stronger HIV suppressive capacity. Thus, such  
35 CD8<sup>+</sup> T cell reprogramming, combined with other available immunomodulators, might  
36 represent a promising strategy for adoptive cell therapy in the search for an HIV-1 cure.

37

38 **Keywords:** CD8<sup>+</sup> T cell; reprogramming; stemness; HIV-1; mTORC; immunotherapy.

39

40

41

42

## 43 INTRODUCTION

44

45 For activation and differentiation, CD8<sup>+</sup> T cells require T cell receptor (TCR) signals  
46 provided by peptide/major histocompatibility complex class I, together with costimulation, and  
47 cytokines. The amount and duration of these signals influence the priming and fate of memory  
48 CD8<sup>+</sup> T cells (1). Human immunodeficiency virus type 1 (HIV-1) infection is an example of the  
49 different outcomes a CD8<sup>+</sup> T cell can reach according to the quality of the priming received  
50 early after infection. For instance, HIV-1 controllers (HICs), who represent less than 0.5% of  
51 people living with HIV-1, control viremia for long periods in the absence of antiretroviral  
52 therapy (ART), and such control is associated with strong HIV-specific CD8<sup>+</sup> T cell responses  
53 (2, 3). Compelling studies indicate that HIV-specific CD8<sup>+</sup> T cells from HICs exhibit stemness  
54 properties, high survival, proliferative potential, and polyfunctionality upon antigen stimulation  
55 (4–7). Recently, we demonstrated that HIV-specific central memory CD8<sup>+</sup> T cells from HICs  
56 have a stem-like transcriptional program, characterized by enhanced polyfunctionality and  
57 survival, compared with cells from non-controllers on ART (8). Moreover, we reported that  
58 early in primary simian immune deficiency virus (SIV) infection there is a divergence in the  
59 memory compartment of SIV-specific CD8<sup>+</sup> T cells of macaques that naturally controlled or  
60 did not control infection later in the chronic phase. In this animal model, SIV controllers  
61 developed stem-like SIV-specific CD8<sup>+</sup> T cells, which preceded the optimal maturation of the  
62 CD8<sup>+</sup> T cell response (i.e., acquisition of SIV-suppressive properties) during infection (9).  
63 Contrary to cells from HICs or SIV controllers, virus-specific memory CD8<sup>+</sup> T cells from non-  
64 controllers exhibit an effector-like and exhausted profile, limited survival capacity, and poor  
65 antiviral potential throughout infection (8–10). Overall, these observations are consistent with  
66 tuned priming of virus-specific CD8<sup>+</sup> T cells early after infection in natural controllers,  
67 promoting long-lived stem-like memory responses that mature throughout infection, whereas

68 there is a skewed or non-regulated CD8<sup>+</sup> T cell priming in non-controllers that promotes short-  
69 lived effector-like responses.

70

71 In part, the stem-like profile of memory CD8<sup>+</sup> T cells is mediated by the transcription factor  
72 TCF-1, a downstream component of the Wnt/ $\beta$ -catenin pathway (11). As such, TCF-1  
73 regulates stemness properties of CD8<sup>+</sup> T cells, including longevity, self-renewal, and the  
74 potential to differentiate into multiple subsets (12). Evidence from chronic infection models  
75 indicates that stem-like memory TCF-1<sup>+</sup> CD8<sup>+</sup> T cells have an enhanced capacity to contain  
76 infection and respond to secondary viral challenges (13–15). Fittingly, we and others have  
77 demonstrated that virus-specific CD8<sup>+</sup> T cells from HIV-1 and SIV controllers exhibit higher  
78 levels of TCF-1 compared with cells from non-controllers (7, 9, 16), further suggesting that  
79 stem-like memory cells exert a protective role in HIV-1/SIV infections.

80

81 Several metabolic cues, such as the mammalian target of rapamycin complex (mTORC)  
82 1 and 2, also regulate CD8<sup>+</sup> T cell fate, longevity, and effector functions (17). Constitutive  
83 activation of the mTORC1 pathway results in terminal differentiation of CD8<sup>+</sup> T cells and lack  
84 of long-term memory, whereas inhibition of mTORC2 leads to excessive activation and cell  
85 death (18). Accordingly, mTORC1 inhibition with rapamycin increases the number, quality,  
86 and survival of stem-like memory CD8<sup>+</sup> T cells (19, 20). In line with those data, we previously  
87 showed that HIV-specific memory CD8<sup>+</sup> T cells from HICs maintain metabolic plasticity and  
88 preferential activation of the mTORC2 pathway, whereas cells from non-controllers are more  
89 dependent on glycolysis and mTORC1 (8). Thus, the ability to use diverse metabolic  
90 resources, as well as the suitable engagement of mTORC1 and 2 pathways, contribute to the  
91 enhanced functionality and longevity of memory HIV-specific CD8<sup>+</sup> T cells from HICs.

92

93        Having identified some signaling pathways and metabolic cues that appear important for  
94 natural HIV-1/SIV control, we hypothesized that reprogramming of HIV-specific CD8<sup>+</sup> T cells  
95 from non-controllers to exhibit characteristics of natural controllers could boost their antiviral  
96 potential. We recently showed that metabolic reprogramming with IL-15 increases  
97 mitochondrial respiration in CD8<sup>+</sup> T cells from non-controllers, contributing to improve their  
98 viral-suppressive capacity *ex vivo* (8). In the present study, we evaluated the potential of CD8<sup>+</sup>  
99 T cell reprogramming for inducing stem-like properties in cells derived from non-controller  
100 individuals, via the manipulation of the TCF-1 and mTORC pathways. We found that, after  
101 reprogramming, virus-specific CD8<sup>+</sup> T cells from non-controllers acquire phenotypic,  
102 transcriptional, metabolic, and functional attributes associated with natural control of HIV-1  
103 infection. Our results shed light on the potential of such CD8<sup>+</sup> T cell reprogramming as novel  
104 therapeutics in the search for an HIV-1 cure.

## 105 **RESULTS**

106

### 107 **CD8<sup>+</sup> T cell reprogramming towards a stem-like memory profile**

108 To test the hypothesis that CD8<sup>+</sup> T cell reprogramming can invigorate stem-like  
109 properties, we used the glycogen synthase kinase-3 (GSK3) inhibitor 6-Bromoindirubin-3'-  
110 oxime (BIO), which modulates pathways involved in the generation and maintenance of stem-  
111 like CD8<sup>+</sup> T cells, such as Wnt/ $\beta$ -catenin and mTORC2 (12), that we and others have found  
112 to be upregulated in CD8<sup>+</sup> T cells from natural controllers (7, 8, 16). We first characterized  
113 the effect of BIO-mediated reprogramming on bulk CD8<sup>+</sup> T cells from people without HIV in  
114 terms of the memory phenotype (Supplementary Fig. 1A). Of note, we performed dose-effect  
115 experiments to establish the optimal dose and time for BIO treatment. We chose 3  $\mu$ M and 12  
116 hs incubation because under these conditions we observed the highest effects on the  
117 expression of representative phenotypic markers, and no drug-induced cellular toxicity  
118 (Supplementary Fig. 1B). Treatment with BIO (in the absence of further stimulation) was  
119 accompanied by upregulation of surface expression of CCR7 and CD27 (Figure 1A).  
120 Accordingly, we observed an enrichment of CD8<sup>+</sup> T cells with a less-differentiated stem cell  
121 memory (TSCM) and central memory (TCM) phenotype, and a decrease of more-  
122 differentiated effector memory (TEM), and terminal effector (TTE) cells (Figure 1A-C). We  
123 confirmed the effect of the GSK3 inhibitor by the enhanced expression of TCF-1 (Figure 1D).  
124 To confirm that these changes were related to the regulation of GSK3 activity, we also  
125 assessed the impact of TWS119, another GSK3 inhibitor previously used to promote stem-  
126 like memory CD8<sup>+</sup> T cells (21). The treatment with both GSK3 inhibitors under parallel  
127 experimental conditions induced CCR7, CD27, and TCF-1 (Supplementary Fig 1C), increase  
128 of TSCM and TCM cells, and decrease of TEM cells (Supplementary Fig. 1D). However, BIO



129 consistently showed a greater effect than TWS119 (Supplementary Fig. 1C and D) and was  
130 used throughout the study. These results confirm that transient exposure to a GSK3 inhibitor,  
131 hereinafter referred to as CD8<sup>+</sup> T cell reprogramming, promotes a memory-like phenotype in  
132 CD8<sup>+</sup> T cells.

133

134 We wondered whether reprogrammed CD8<sup>+</sup> T cells maintained their memory-like  
135 profile upon activation. Following anti-CD3/CD28 stimulation, reprogrammed CD8<sup>+</sup> T cells,  
136 when compared to cells in the control condition, exhibited lower expression of the activation  
137 markers HLA-DR and CD38, the inhibitory receptors PD-1, LAG-3, and TIM-3, and the  
138 transcription factors T-bet and BLIMP-1, which are associated with an effector CD8<sup>+</sup> T cell  
139 profile (Figure 1E and Supplementary Fig. 1E) (22). On the contrary, reprogrammed CD8<sup>+</sup> T  
140 cells maintained higher levels of the transcription factors BCL-6 and TCF-1, associated with  
141 a memory profile (23, 24), as well as CD127, critical for CD8<sup>+</sup> T cell survival (Figure 1E) (25).  
142 In addition, reprogrammed cells exhibited higher expression of TOX. While this transcription  
143 factor regulates the transcriptional and epigenetic signature of exhausted T cells (26), it also  
144 restricts terminal effector differentiation and allows the persistence of antiviral CD8<sup>+</sup> T cells  
145 (27, 28), and is found in polyfunctional memory CD8<sup>+</sup> T cells (16). Consistent with the higher  
146 expression of CD127 and restriction of T-bet, reprogrammed CD8<sup>+</sup> T cells showed lower  
147 levels of activation-induced cell death than cells in the control condition (Figure 1F). The  
148 effects of CD8<sup>+</sup> T cell reprogramming were also observed in the setting of a lower and higher  
149 TCR-mediated stimulation with anti-CD3/CD28 ± ICAM-1 (29) since reprogrammed CD8<sup>+</sup> T  
150 cells maintained lower frequencies of T-bet<sup>+</sup> cells than non-reprogrammed cells  
151 (Supplementary Fig. 1F and G).

152

153 **Reprogrammed CD8<sup>+</sup> T cells show enhanced polyfunctionality**

154 As reprogramming of CD8<sup>+</sup> T cells decreased the proportion of effector cells and  
155 restricted cell activation, we wondered whether reprogrammed CD8<sup>+</sup> T cells could acquire  
156 functional capacity. Consistent with the restriction of an effector-like transcriptional program,  
157 reprogrammed total CD8<sup>+</sup> T cells had lower expression of granzyme B and IL-2 than non-  
158 reprogrammed cells upon stimulation with anti-CD3/CD28 , although there was no change in  
159 IFN- $\gamma$  production (Figure 1G). In contrast, there was a marked increase in the capacity of  
160 reprogrammed CD8<sup>+</sup> T cells to produce TNF- $\alpha$  and overall increased polyfunctionality (Figure  
161 1G and H). We did not observe significant differences between non-reprogrammed vs  
162 reprogrammed cells in the expression of the effector molecules on cells responding to  
163 stimulation on a per cell basis (e.g. fluorescence intensity of granzyme B in granzyme B<sup>+</sup> cells),  
164 (Supplementary Fig. 1H). Higher polyfunctionality was also observed after stimulation with  
165 anti-CD3/CD28 + ICAM-1 (Supplementary Fig. 1I).

166  
167 We also assessed the impact of CD8<sup>+</sup> T cell reprogramming on the proliferative  
168 capacity and effector maturation upon sequential polyclonal re-stimulation. Interestingly,  
169 reprogramming did not affect CD8<sup>+</sup> T cell capacity to execute 1-3 division cycles but  
170 prevented extensive proliferation ( $\geq 4$  cell divisions) and maintained a higher proportion of  
171 quiescent cells (Supplementary Fig. 1J). This pattern of regulated proliferation of  
172 reprogrammed cells was associated with a lower coexpression of PD-1, LAG-3, TIM3, and  
173 TIGIT on CD8<sup>+</sup> T cells after re-stimulation (Supplementary Fig. 1K). Notably, reprogramming  
174 did not irreversibly arrest effector maturation of less-differentiated TCM and transitional  
175 memory (TTM) cells since these subsets could readily upregulate T-bet under the re-  
176 stimulation setting (Supplementary Fig. 1L). Collectively, these results indicate that CD8<sup>+</sup> T

177 cell reprogramming induces TNF- $\alpha$  production and enhanced polyfunctionality, while  
178 maintaining responsiveness to recall.

179

## 180 **Reprogramming modifies the functional properties and transcriptional signature of all** 181 **CD8<sup>+</sup> T cell memory subsets**

182 We asked if the changes induced by cell reprogramming were related to phenotype  
183 conversion between CD8<sup>+</sup> T cell subpopulations or were intrinsic to each subset. To solve  
184 this issue, we isolated TCM, TTM, TEM, and TTE CD8<sup>+</sup> T cells and treated them with the  
185 GSK3 inhibitor, followed by resting or stimulation with anti-CD3/CD28. In basal conditions,  
186 cell reprogramming caused the upregulation of CCR7 and CD27 in all cell subsets (Figure  
187 2A). Thus, the enrichment in less-differentiated cells observed after CD8<sup>+</sup> T cell  
188 reprogramming (Figure 1A-C) is most likely the result of the conversion of CD27<sup>-</sup> and CCR7<sup>-</sup>  
189 cells into CD27<sup>+</sup> and CCR7<sup>+</sup> subsets. In addition, reprogramming further enhanced the  
190 expression of CD28 and TCF-1 in TCM and TTM cells (Figure 2A), while preventing the loss  
191 of CD127 and limiting the upregulation of T-bet upon stimulation of CD8<sup>+</sup> T cell memory  
192 subsets (Figure 2B). Notably, reprogramming of TCM and TTM cells restrained the  
193 expression of granzyme B, IFN- $\gamma$ , and IL-2, but TEM and TTE cells maintained these effector  
194 properties (Figure 2C). As was observed with bulk CD8<sup>+</sup> T cells, all reprogrammed CD8<sup>+</sup> T  
195 cell subsets exhibited an increased TNF- $\alpha$  production (Figure 2C).

196

197 To better characterize the changes induced in reprogrammed CD8<sup>+</sup> T cells, we  
198 performed a gene expression analysis of sorted memory cells, analyzing 96 genes associated  
199 with CD8<sup>+</sup> T cell function, differentiation, metabolism, and survival (see Supplementary Table  
200 1). A principal component analysis (PCA) focused on TCM cells showed that reprogrammed

201 and non-reprogrammed cells had a distinct gene expression profile (Figure 2D). In basal  
202 conditions, compared with non-reprogrammed cells, reprogrammed TCM cells exhibited  
203 lower levels of *IFNG*, *BATF*, *IFNGR1*, and *GZMK* genes, which are associated with an effector  
204 lineage (30, 31), as well as *CD8A*, *CD244*, and *HAVCR2* (which codifies for TIM3), which are  
205 associated with CD8<sup>+</sup> T cell activation and exhaustion (32) (Figure 2E). Reprogrammed CD8<sup>+</sup>  
206 T cells exhibited in contrast a gene profile suggestive of metabolic quiescence (33), with lower  
207 levels of key metabolic regulators active during T cell activation, including *MLST8* (which  
208 codifies for MTOR Associated Protein, LST8 Homolog; required for mTORC pathway  
209 activation (34)), *ESRRA* (which codifies for Estrogen-related receptor  $\alpha$ ; metabolic regulator  
210 of effector T cells (35)), *GSL* and *GSL2* (which codify for glutaminase 1 and 2, respectively  
211 (36)), and *PRKAA1* (which codifies for AMP-activated protein kinase; important regulator of  
212 cell catabolic pathways (37)) (Figure 2E). Importantly, after anti-CD3/CD28 stimulation,  
213 reprogrammed TCM cells had higher levels of the antiapoptotic gene *BCL2* than non-  
214 reprogrammed cells, and lower levels of effector-associated genes *FASLG*, *HAVCR2*, and  
215 *GZMB*, as well as *PRKAA1* (Figure 2E). The gene expression profile in reprogrammed TTM,  
216 TEM, and TTE was also modified by reprogramming (Supplementary Fig. 2), and, among  
217 others, higher expression of *BCL2* and the mTORC2-related gene *CDC42* was observed in  
218 these memory subsets (Figure 2E, Supplementary Fig. 2, and Supplementary Table 2),  
219 explaining in part the improved survival capacity of reprogrammed CD8<sup>+</sup> T cells.

220

221 **The stem-like profile and polyfunctionality of reprogrammed CD8<sup>+</sup> T cells is associated**  
222 **with the downregulation of anabolic metabolism and the mTORC1 pathway**

223 Considering that regulation of cell metabolism and mTORC pathways is a  
224 characteristic of memory-like CD8<sup>+</sup> T cells (38), as we and others have reported for cells from  
225 HICs (8, 39), and that CD8<sup>+</sup> T cell reprogramming readily modulated metabolism-related

226 genes, we performed functional assays to evaluate the metabolic profile of reprogrammed  
227 cells. After anti-CD3/CD28 stimulation, non-reprogrammed cells increased their 2-NBDG and  
228 BODIPY labelling (commonly used as indicators of glucose and lipid uptake), augmented the  
229 mitochondrial mass, and the production of reactive oxygen species (ROS) (Figure 3A and B),  
230 a profile characteristic of recently activated T cells (33). However, reprogrammed CD8<sup>+</sup> T  
231 cells showed lower levels of each of these metabolic parameters (Figure 3A and B),  
232 consistent with reduced anabolic metabolism.

233

234 We next focused on the mTORC pathways and evaluated their activation by analyzing  
235 the phosphorylation of ribosomal S6 (pS6 Ser235/236) and AKT (pAKT Ser473) proteins,  
236 markers of activation of mTORC1 and mTORC2, respectively (40). Upon activation in control  
237 conditions, CD8<sup>+</sup> T cells upregulated pS6 in parallel with pAKT (pS6<sup>+</sup> pAKT<sup>+</sup> cells; Figure 3C).  
238 Consistent with the reported modulation of the mTORC1 pathway by GSK3 inhibitors (20),  
239 reprogrammed CD8<sup>+</sup> T cells had less upregulation of pS6 (Figure 3C). Notably,  
240 reprogrammed CD8<sup>+</sup> T cells had higher levels of pS6<sup>-</sup> pAKT<sup>+</sup> (Figure 3C), confirming that  
241 reprogrammed cells maintained a relative metabolic quiescence supported by preferential  
242 upregulation of the mTORC2 pathway. As shown above, reprogrammed CD8<sup>+</sup> T cells had  
243 increase capacity to produce TNF- $\alpha$  upon polyclonal stimulation. When analyzing IFN- $\gamma$  and  
244 IL-2 production among TNF- $\alpha$ -producing CD8<sup>+</sup> T cells, two major subpopulations were  
245 identified: IFN- $\gamma$ <sup>+</sup> IL-2<sup>+</sup> and IFN- $\gamma$ <sup>-</sup> IL-2<sup>-</sup>, the latter corresponding to cells producing TNF- $\alpha$  only  
246 and being increased among reprogrammed cells (Figure 3D). In keeping with our previous  
247 studies on cells from HICs (8), the production of TNF- $\alpha$  by reprogrammed cells was less  
248 dependent on mTORC1. This was particularly the case for cells only producing TNF- $\alpha$ , since  
249 the proportion of pS6<sup>+</sup> cells was lower in this subset relative to cells co-producing IFN- $\gamma$  and

250 IL-2 (Figure 3D). Altogether, these data indicate that the stem-like profile and polyfunctionality  
251 observed in reprogrammed CD8<sup>+</sup> T cells are linked to the active regulation of anabolic  
252 metabolism, mTORC1 inhibition, and preferential engagement of mTORC2. Our data also  
253 highlight the differential role of mTORC pathways on the regulation of CD8<sup>+</sup> T cell effector  
254 functions.

255

### 256 **Reprogramming of HIV-specific CD8<sup>+</sup> T cells promotes polyfunctionality, survival, and** 257 **expansion**

258 Our results on polyclonally-stimulated cells from people without HIV indicated that  
259 reprogramming improves several functional capacities of CD8<sup>+</sup> T cells, without impairing  
260 others. However, HIV-specific CD8<sup>+</sup> T cells from non-controllers have a biased program  
261 characterized by exhaustion, low survival, and poor antiviral potential (8). Thus, we explored  
262 if HIV-specific CD8<sup>+</sup> T cells from non-controller individuals (people on ART to suppress  
263 viremia [Supplementary Table 3]) can also benefit from reprogramming and acquire  
264 properties found in HIV-specific CD8<sup>+</sup> T cells associated with natural control of infection. First,  
265 we evaluated the effect of reprogramming on the phenotype of CD8<sup>+</sup> T cells labeled with HIV-  
266 specific HLA dextramers. In line with the results on total CD8<sup>+</sup> T cells from people without  
267 HIV, a Uniform Manifold Approximation and Projection (UMAP) analysis focused on HIV  
268 dextramer<sup>+</sup> cells revealed enrichment of populations with a less-differentiated phenotype after  
269 reprogramming (Figure 4A), linked to the upregulation of CCR7, CD27, and TCF-1 (Figure  
270 4B), increase in the proportions of naïve/TSCM and TCM cells, and decrease of TEM and  
271 TTE cells (Figure 4C).

272

273 Next, we evaluated the functionality of HIV-specific CD8<sup>+</sup> T cells, detected by the  
274 peptide-induced production of IFN- $\gamma$ , IL-2, TNF- $\alpha$ , or by the expression of the degranulation

275 marker CD107a. Reprogrammed CD8<sup>+</sup> T cells contained a significantly higher frequency of  
276 total HIV-specific responses (Figure 4D), that were enriched in TCM cells (Figure 4E).  
277 Instead, non-reprogrammed cells were mostly TEM and TTE cells (Figure 4E). Notably,  
278 higher production of TNF- $\alpha$  by reprogrammed cells was observed in terms of both frequency  
279 (Supplementary Fig. 3A) and level of expression (Figure 4F) in HIV-specific CD8<sup>+</sup> T cells,  
280 whereas there were no differences in the levels of CD107a, IFN- $\gamma$ , granzyme B, and IL-2  
281 (Figure 4F). An overall increased polyfunctionality was observed in reprogrammed HIV-  
282 specific CD8<sup>+</sup> T cells relative to non-reprogrammed cells (Figure 4G). Of note, the survival  
283 capacity of reprogrammed HIV-specific cells was higher relative to non-reprogrammed cells  
284 (Figure 4H and Supplementary Fig. 3B), in agreement with our observation that  
285 reprogramming induced the upregulation of anti-apoptotic factors (Figure 2E). This resulted  
286 in enhanced survival of HIV-specific cells over 6 days culture in the setting of sequential  
287 peptide re-stimulation (Figure 4I).

288

289 We next wondered whether the effects of CD8<sup>+</sup> T cell reprogramming are restricted to  
290 HIV-specific cells or also impact other antigen specific cells, such as those specific of human  
291 cytomegalovirus (HCMV). When analyzing HCMV-specific CD8<sup>+</sup> T cells from people without  
292 HIV we did not observe an increase in the total frequency of HCMV-specific CD8<sup>+</sup> T cells after  
293 reprogramming (Supplementary Fig. 4A and B). Nonetheless, reprogrammed HCMV-specific  
294 were enriched in a TCM phenotype (Supplementary Fig. 4C) and had higher TNF- $\alpha$   
295 expression relative to non-reprogrammed cells (Supplementary Fig. 4D). We next performed  
296 parallel stimulations with HCMV pp65 or HIV Gag peptides and evaluated the phenotype and  
297 function of antigen-specific cells from the same individuals with HIV. In line with our previous  
298 results (Figure 4F), we did not observe significant differences in the frequencies of CD107a<sup>+</sup>

299 or IFN- $\gamma$ <sup>+</sup> HCMV or HIV-specific CD8<sup>+</sup> T cells between reprogrammed versus non-  
300 reprogrammed cells (Supplementary Fig. 4E). Instead, we readily observed an increase of  
301 TNF- $\alpha$ <sup>+</sup> HCMV and HIV-specific CD8<sup>+</sup> T cells in reprogrammed cells relative to non-  
302 reprogrammed cells. The enhancement appeared stronger for HIV-specific cells, since the  
303  $\Delta$  change in TNF- $\alpha$  production by reprogrammed/non-reprogrammed cells was higher in HIV-  
304 specific versus HCMV-specific cells (Supplementary Fig. 4F). Overall, these data suggest  
305 that the effects of reprogramming might be stronger in HIV-specific cells than in HCMV-  
306 specific cells, which may be related to metabolic and functional differences in these antigen-  
307 specific populations in the same host (8, 41).

308 Collectively, these results indicate that reprogramming of HIV-specific CD8<sup>+</sup> T cells  
309 from non-controllers promotes a quantitatively and qualitatively superior response to antigen  
310 stimulation, reflected in higher functionality, survival, and expansion capacity, which are  
311 features observed in cells from natural HIV-1 controllers.

### 312 313 **Metabolic plasticity restored in reprogrammed HIV-specific CD8<sup>+</sup> T cells**

314 We next assessed whether reprogramming could improve the marked dependency on  
315 mTORC1 and glycolysis that characterizes HIV-specific CD8<sup>+</sup> T cells from HIV-1 non-  
316 controllers (8). Stimulation of non-reprogrammed cells from non-controllers with HIV-1 Gag  
317 peptides resulted in upregulation of pS6 (Supplementary Fig. 5A), both alone and together  
318 with pAKT (Figure 4J). In contrast, reprogrammed HIV-specific CD8<sup>+</sup> T cells had lower  
319 proportions of pS6<sup>+</sup> pAKT<sup>-</sup> cells (Figure 4K). A significantly lower expression of pS6 was also  
320 observed on a per-cell basis in reprogrammed HIV-specific CD8<sup>+</sup> T cells (Figure 4K and  
321 Supplementary Fig. 5A). In contrast, we did not observe significant differences in the intensity  
322 of pAKT in reprogrammed cells (Figure 4J and K). These data indicate that reprogrammed



323 HIV-specific CD8<sup>+</sup> T cells had a diminished dependency on mTORC1 for supporting a strong  
324 antigen-induced response, while preserving mTORC2 activation to exert their functions. We  
325 additionally evaluated glucose dependency of reprogrammed HIV-specific CD8<sup>+</sup> T cells in an  
326 assay where Gag peptide stimulation was performed in medium with versus without glucose  
327 (8). Glucose deprivation decreased the frequency of total HIV-specific cells at comparable  
328 levels in reprogrammed versus non-reprogrammed cells (Supplementary Fig. 5B and C).  
329 However, reprogrammed cells maintained higher production of TNF- $\alpha$  despite glucose  
330 deprivation (Supplementary Fig. 5D). Altogether, these data indicate that reprogramming of  
331 HIV-specific cells from non-controllers promotes metabolic plasticity and decreases metabolic  
332 restrictions.

### 333

### 334 **Reprogramming reinvigorates CD8<sup>+</sup> T cells to suppress HIV-1 replication**

335 To further elucidate the antiviral potential of reprogrammed CD8<sup>+</sup> T cells, we evaluated  
336 the capacity of non-stimulated cells from non-controller individuals under ART to suppress  
337 HIV-1 infection of autologous CD4<sup>+</sup> T cells (42). According to our previous studies (8, 10, 43),  
338 non-reprogrammed CD8<sup>+</sup> T cells from HIV-1 non-controllers under ART exhibited poor  
339 capacity to counteract HIV-1 infection when co-cultured with infected CD4<sup>+</sup> T cells; in contrast,  
340 reprogramming strongly improved the capacity of CD8<sup>+</sup> T cells to suppress HIV-1 infection  
341 (Figure 5A and B, and Supplementary Fig. 6A). It should be noted that we cannot exclude  
342 that, at the time of starting the coculture, the frequency of HIV-specific CD8<sup>+</sup> T cells was  
343 higher upon reprogramming, due to the promotion of the survival capacity of the cells.  
344 However, we did not observe differences in the frequency of IFN- $\gamma$ <sup>+</sup> CD8<sup>+</sup> T cells (presumably  
345 HIV-specific) between reprogrammed and non-reprogrammed cells at the end of the coculture  
346 (day 7; Figure 5C), but reprogrammed IFN- $\gamma$ <sup>+</sup> CD8<sup>+</sup> T cells maintained a memory-like profile,

347 with higher expression of CCR7 and decreased expression of the inhibitory receptors PD-1  
348 and LAG-3 (Figure 5D and Supplementary Fig. 6B). Therefore, our data indicate that  
349 reprogramming of CD8<sup>+</sup> T cells from non-controllers strengthens their direct anti-HIV potential  
350 while restricting the acquisition of a terminally differentiated, exhausted program.

351

### 352 **Reprogrammed CD8<sup>+</sup> T cells respond better to homeostatic $\gamma$ -chain cytokines**

353 The long-term maintenance of memory T cells requires an optimal response to the  $\gamma$ -  
354 chain cytokines IL-7 and IL-15 for self-renewal (44). Thus, we evaluated how reprogramming  
355 impacted the capacity of CD8<sup>+</sup> T cells to respond to these homeostatic cytokines. We have  
356 shown that reprogrammed bulk CD8<sup>+</sup> T cells were characterized by higher levels of CD127  
357 (IL-7R $\alpha$  chain; Figure 1E). We also found that reprogrammed CD8<sup>+</sup> T cells had higher  
358 expression of CD122 (IL-2R $\beta$  chain, component of the IL-15 receptor) and the IL-15R $\alpha$  chain  
359 CD215 (Supplementary Fig. 7A and B), as well as a higher proportion of cells co-expressing  
360 the transcription factor Eomesodermin (Eomes) and CD122 (Figure 6A). This may be related  
361 to previous observations showing that TCF-1 regulates the expression of Eomes, which in  
362 turn promotes CD122 (24).

363

364 The increased expression of IL-7 and IL-15 receptors in reprogrammed bulk CD8<sup>+</sup> T  
365 cells from people without HIV was reflected in augmented proliferation in response to both  
366 cytokines when compared to non-reprogrammed cells (Figure 6B). As expected, the  
367 proliferative potential was higher in naïve/TSCM and TCM cells than in more differentiated  
368 cells (Figure 6B). Reprogramming also improved the proliferative response to IL-15 of HIV  
369 dextramer<sup>+</sup> cells from HIV-1 non-controllers (Figure 6C and D). Finally, the maturation of the  
370 effector response induced by IL-15 in terms of upregulation of T-bet was comparable between

371 reprogrammed and non-reprogrammed cells (Supplementary Fig. 7C). Overall, our results  
372 show that CD8<sup>+</sup> T cell reprogramming improves the response to homeostatic  $\gamma$ -chain  
373 cytokines in cells with otherwise diminished capacity.

374

## 375 **DISCUSSION**

376

377 We report that reprogramming of HIV-specific CD8<sup>+</sup> T cells from HIV-1 non-controllers  
378 via GSK3 inhibition confers them higher polyfunctionality, survival, expansion capacity,  
379 diminished dependency on mTORC1 and glucose, better responsiveness to  $\gamma$ -chain  
380 cytokines, and strong HIV-1 suppressive capacity. These characteristics have been  
381 previously associated with efficient responses in natural HIV-1 controllers (4–8). Thus, such  
382 CD8<sup>+</sup> T cell reprogramming represents a promising option to enhance the efficacy of cell-  
383 based therapies for HIV-1 infection.

384

385 Our choice of targeting GSK3 was based on the implication of this molecule in the  
386 modulation of several intracellular pathways that we have identified to be of potential  
387 relevance in virus-specific CD8<sup>+</sup> T cells from HIV-1 (8) and SIV natural controllers (9). BIO  
388 and TWS119, the two molecules that we used here, are highly selective inhibitors of GSK3  
389 and induce the activation of the Wnt/ $\beta$ -catenin/TCF-1 pathway (45). Higher TCF-1 expression  
390 is a characteristic of virus-specific CD8<sup>+</sup> T cells in HIV-1 and SIV controllers (7, 9, 16), and  
391 the intensification of its function promotes CD8<sup>+</sup> T cell stemness, which associates with potent  
392 viral and tumor control (7, 46). It is also well described that stem-like memory TCF-1<sup>+</sup> CD8<sup>+</sup>  
393 T cells have strong antiviral potential and therapeutic benefit (13–15, 47, 48), related to their  
394 longevity and enhanced ability to expand and differentiate into effector subsets (48, 49). In

395 addition, GSK3 interacts with the mTOR signaling network (50), and its inhibition promotes  
396 the activation of the mTORC2 pathway (51). The mTORC2 pathway promotes the generation  
397 of memory CD8<sup>+</sup> T cells (52) and is preferentially upregulated in HIV-specific CD8<sup>+</sup> T cells  
398 from HICs (8).

399

400 According to the effects of GSK3 inhibition, in our study, we show that CD8<sup>+</sup> T cell  
401 reprogramming promoted the expression of TCF-1, a TCM and TSCM phenotype, as well as  
402 restrained effector differentiation. Reprogrammed CD8<sup>+</sup> T cells also regulated proliferation to  
403 maintain quiescence, and to limit the consequences of excessive activation (21, 53, 54).  
404 Correspondingly, reprogrammed CD8<sup>+</sup> T cells shifted their transcriptomic profile towards a  
405 program of quiescence and survival, and downregulated several genes associated with  
406 anabolic metabolism (55), reflected in lower glucose and lipid consumption, and mitochondrial  
407 activity. These data are in line with previous studies showing the critical role of metabolism  
408 on CD8<sup>+</sup> T cell effector versus memory fate (56, 57), and the quiescent profile of less  
409 differentiated subsets (49, 58). Remarkably, both polyclonal and HIV-specific reprogrammed  
410 CD8<sup>+</sup> T cells showed lower activation of mTORC1, and a predilection for mTORC2 pathway  
411 activation to sustain their activities. Moreover, reprogrammed HIV-specific CD8<sup>+</sup> T cells  
412 depended less on glucose. Such metabolic plasticity is also found in cells from HICs and may  
413 be particularly helpful in hostile metabolic environments such as tissues, with infected cells  
414 competing for nutrients (59) and high antigen load and inflammation impacting the survival  
415 and function of CD8<sup>+</sup> T cells (60). The modulation of metabolism and the induction of a stem-  
416 like profile are likely related and synergize to improve CD8<sup>+</sup> T cell antiviral potential, even in  
417 settings of persistent or strong antigen stimulation. Indeed, the maintenance of a stem-like  
418 profile and less effector differentiation and immune exhaustion were associated with a  
419 stronger HIV-1 suppression by reprogrammed CD8<sup>+</sup> T cells. These properties exhibited by

420 reprogrammed HIV-specific CD8<sup>+</sup> T cells might contribute to long-term viral control in vivo.  
421 Supporting this notion, stem-like SIV-specific CD8<sup>+</sup> T cells are long-term maintained and are  
422 linked to the natural control of infection (9).

423

424 We found that reprogramming did not affect all CD8<sup>+</sup> T cells uniformly. Although BIO  
425 induced very similar effects globally on CD8<sup>+</sup> T cells, reprogramming seemed to have the  
426 strongest enhancing effect of the activities of HIV-specific CD8<sup>+</sup> T cells from non-controllers  
427 when compared to cells responding to polyclonal stimulation or HCMV peptides. We have  
428 previously shown that HCMV and HIV-specific cells from HICs are relatively similar in terms  
429 of memory metabolic program (8). In contrast, HIV-specific cells from non-controllers have an  
430 effector-like and exhausted profile (8, 61, 62), and such a biased program can be found even  
431 among the TCM population (8). These divergent signatures in cells from controllers and non-  
432 controllers could be related to the TCR signaling and priming signals they received in vivo  
433 early after infection (9), which may be exacerbated by the persistence of high amounts of  
434 antigen and inflammation in non-controller individuals. Thus, it was expected that HIV-specific  
435 CD8<sup>+</sup> T cells derived from non-controllers benefited the most from the effects of  
436 reprogramming when compared to better-fitted HCMV-specific cells. Along these lines, our  
437 results show that the skewed program of HIV-specific CD8<sup>+</sup> T cells from non-controllers is at  
438 least partially reversible.

439

440 Our results also show that not all CD8<sup>+</sup> T cells activities are equally regulated by  
441 metabolic pathways. Observations in one of our previous studies suggested that  
442 polyfunctionality, and in particular TNF- $\alpha$  production, might depend on the mTORC2 pathway  
443 (8). This aspect was confirmed here. We observed a selective increase in the production of

444 TNF- $\alpha$  by reprogrammed CD8<sup>+</sup> T cells, which was related to the inhibition of mTORC1,  
445 preservation of the mTORC2 pathway, and less dependency on glycolysis. In contrast, IFN- $\gamma$   
446 and IL-2 production was associated with mTORC1 activation. In keeping with our results,  
447 previous studies have demonstrated that TNF- $\alpha$  production is associated with a less-  
448 differentiated CD8<sup>+</sup> T cell profile (63, 64), while the transcription factor NF- $\kappa$ B (regulator of  
449 TNF- $\alpha$  expression) is active in stem-like CD8<sup>+</sup> T cells (48, 65), suggesting a role of this  
450 signaling pathway as a regulator of this subset. The underlying mechanism of greater TNF- $\alpha$   
451 production by reprogrammed CD8<sup>+</sup> T cells might be related to epigenetic modifications and/or  
452 posttranscriptional events (64, 66), that deserve further study. Moreover, although further  
453 studies are necessary to fully elucidate this aspect, our data suggest that the production of  
454 TNF- $\alpha$  in the absence of mTORC1 activity (pS6 expression) could serve as an additional  
455 marker of stem-like memory CD8<sup>+</sup> T cells. In the context of HIV-1 control, TNF- $\alpha$  might help  
456 to inhibit HIV replication, as has previously been shown in monocytes and macrophages (67,  
457 68), and its production, together with other soluble factors, may contribute to provide an  
458 antiviral environment while CD8<sup>+</sup> T cells are arrested to killed target cells (69). Interestingly,  
459 a previous study showed that the cytotoxic capacity of HIV-specific CD8<sup>+</sup> T cells is enhanced  
460 in cells producing both IFN- $\gamma$  and TNF- $\alpha$  (70). However, this did not appear to be related to a  
461 direct cytotoxic effect of TNF- $\alpha$ . Simultaneous production of IFN- $\gamma$  and TNF- $\alpha$  rather revealed  
462 a subset of cells with qualitatively superior cytotoxic potential (70). Moreover, TNF- $\alpha$  has also  
463 been shown to reverse latency of provirus in persistently infected cells (71, 72). This might  
464 be relevant in vivo, where local production of TNF- $\alpha$  may reveal the presence of latently  
465 infected cells, facilitating their elimination by the cytotoxic activity of the CD8<sup>+</sup> T cells. Thus,  
466 TNF- $\alpha$  production and polyfunctionality are a feature of the stem-like profile in HIV-specific  
467 CD8<sup>+</sup> T cells promoted by reprogramming, that, together with other functional attributes

468 (including higher survival, proliferative potential, and metabolic plasticity) may collectively  
469 contribute to the augmented antiviral potential observed.

470

471 We propose that reprogramming HIV-specific CD8<sup>+</sup> T cells may be of potential interest  
472 for interventions aiming at HIV-1 remission. Two beneficial effects could be expected: first,  
473 we have shown here that reprogramming reinvigorates the antiviral potential of HIV-specific  
474 CD8<sup>+</sup> T cells; secondly, the promotion of self-renewal and long-term survival of the cells may  
475 improve the therapeutic efficacy of adoptive immunotherapies. Indeed, one of the major  
476 caveats in adoptive immunotherapies is the low persistence of transferred cells, which impairs  
477 the long-term therapeutic efficacy, as has been observed in HIV-1<sup>+</sup> individuals receiving  
478 autologous, ex vivo-expanded HIV-specific CD8<sup>+</sup> T cells (73–75). In line with this notion,  
479 complete cancer regression and persistence of transferred tumor-reactive CD8<sup>+</sup> T cells have  
480 been associated with a stem-like population capable of self-renewal, expansion, and  
481 antitumor responses (76). Of note, CD8<sup>+</sup> T cell reprogramming could be combined with other  
482 interventions to further enhance their antiviral potential. We have previously shown that short  
483 IL-15 treatment of HIV-specific CD8<sup>+</sup> T cells from non-controllers increased their capacity to  
484 mobilize mitochondrial activities and their capacity to suppress HIV-1 infection of CD4<sup>+</sup> T cells  
485 (8). As reprogrammed CD8<sup>+</sup> T cells are more responsive to IL-15 in terms of proliferation and  
486 maturation of their effector profile, we hypothesize that a combined approach may have  
487 synergistic effects.

488

489 A limitation of our study is that all analyses were performed ex vivo. Therefore, it  
490 remains to elucidate the antiviral potential and lifespan of adoptively transferred,  
491 reprogrammed HIV-specific CD8<sup>+</sup> T cells in vivo, considering potential escape mutations,  
492 inflammatory conditions, and the nature of the HIV-1 reservoir. Indeed, a high proportion of

493 latent viruses exhibit escape mutations to evade the CD8<sup>+</sup> T cell response (77), which may  
494 compromise the efficacy of CD8<sup>+</sup> T cell-based cure strategies. However, the superior in vivo  
495 antitumor response of transferred stem-like CD8<sup>+</sup> T cells in human cancer (76), as well as the  
496 enhanced anti-HIV potential exhibited by reprogrammed CD8<sup>+</sup> T cells ex vivo, support the  
497 rationale of exploring this immunotherapy, in combination with other methodologies (such as  
498  $\gamma$ -chain cytokines, or chimeric antigen receptor cells), in the context of HIV-1 infection.  
499 Another limitation in our study is that we only evaluated the impact of reprogramming in CD8<sup>+</sup>  
500 T cells from people with HIV receiving ART, and not from viremic untreated individuals, who  
501 are expected to have more dysfunctional cells. However, individuals under ART would be the  
502 main target population for these immunotherapies given the well-known benefits of treatment  
503 initiation. Moreover, in this study we only analyzed cells derived from blood and not from  
504 tissues. Thus, future studies could evaluate if GSK3 inhibitors also modify the program of  
505 tissue resident memory cells. In addition, in our study we propose the use of reprogramming  
506 with BIO for adoptive cell therapies. Given the multisystemic effects that GSK3-targeting  
507 drugs could have in vivo (78), it remains to be explored the use of other GSK3 inhibitors with  
508 proved clinical safety and tolerability (78, 79), that could be injected systemically to reprogram  
509 CD8<sup>+</sup> T cells in vivo.

510

511 In summary, here we show that HIV-specific CD8<sup>+</sup> T cell pharmacologic  
512 reprogramming into stem-like cells induces several properties associated with natural control  
513 of infection and help to improve the response to immunomodulators. CD8<sup>+</sup> T cell  
514 reprogramming could be used to potentiate the therapeutic efficacy of this cell population in  
515 adoptive transfer strategies, as well as the effect of other immunotherapies, in the search for  
516 an HIV-1 cure or remission or development of therapeutic vaccines. In addition, the benefits



517 of T cell reprogramming could be extended to the context of other chronic viral infections or  
518 tumors where antigen-specific CD8<sup>+</sup> T cells have a skewed and dysfunctional profile.

519 **MATERIALS AND METHODS**

520

521 **Participants**

522 Samples from people without HIV were obtained from the Etablissement Français du  
523 Sang in the context of a collaboration agreement with Institut Pasteur. HIV-1 non-controller  
524 participants (on ART for at least 2 years and undetectable HIV-1 RNA) were recruited in the  
525 context of the ANRS EP36 XII mTOR study or ANRS CO6 PRIMO cohort. Clinical data for  
526 participants included are summarized in Supplementary Table 3. All analyses were done on  
527 cryopreserved PBMCs isolated from blood samples.

528

529 **In vitro reprogramming of CD8<sup>+</sup> T cells**

530 Frozen PBMC were thawed and rested overnight at 37°C, 5% CO<sub>2</sub>, in RPMI 1640  
531 GlutaMAX medium supplemented with 10% fetal calf serum and penicillin/streptomycin  
532 (complete medium). For reprogramming of CD8<sup>+</sup> T cells followed by polyclonal stimulation,  
533 cells were isolated by negative magnetic bead sorting (Stemcell Technologies). For  
534 reprogramming of CD8<sup>+</sup> T cells followed by antigen-specific stimulation, we used PBMC and  
535 magnetically separated CD8<sup>+</sup> T cells and non-CD8<sup>+</sup> T cells (REAl ease<sup>®</sup> CD8 MicroBead Kit;  
536 Miltenyi Biotech). Then, CD8<sup>+</sup> T cells were treated with a GSK3 inhibitor (6-Bromoindirubin-  
537 3'-oxime; BIO; Sigma-Aldrich), at 3 μM, or an equivalent concentration of dimethyl sulfoxide  
538 (DMSO) vehicle control, in complete medium, for 12 hs at 37°C, 5% CO<sub>2</sub>. Non-CD8 cells were  
539 left resting during this time in complete medium. CD8<sup>+</sup> T cells were washed with complete  
540 medium and stimulated with the peptide pool in presence of non-CD8 T cells. To confirm the  
541 effects of BIO, another GSK3 inhibitor, TWS119 (Sigma-Aldrich), was used under similar  
542 conditions (at 3 μM, 12 hs incubation).

543

544 **Polyclonal, antigen-specific, and cytokine stimulation of CD8<sup>+</sup> T cells**

545           After reprogramming, CD8<sup>+</sup> T cells were polyclonally stimulated with plate-bound anti-  
546 CD3 and CD28 antibodies (both at 1 µg/mL; clones OKT3 and CD28.2, respectively; both  
547 from Thermo Fisher), in the presence or absence of human recombinant ICAM-  
548 1/CD54 Fc Chimera Protein (at 50 µg/mL; R&D) and cultured for 48 hs at 37°C, 5% CO<sub>2</sub>,  
549 accordingly. For intracellular cytokine analyses upon polyclonal stimulation, brefeldin A (at 10  
550 µg/mL; Sigma-Aldrich) was added to the cells and incubated during the last 12 hs of culture.  
551 Antigen-specific stimulation was performed by mixing CD8<sup>+</sup> and non-CD8 cells (maintaining  
552 the original cell ratio) and incubating with overlapping peptide pools encompassing HIV-1  
553 consensus subtype B Gag or HCMV pp65 (both at 2 µg/ml; obtained through the National  
554 Institute of Health (NIH) AIDS Reagent Program, Division of AIDS, National Institute of Allergy  
555 and Infectious Diseases, NIH, catalog numbers 12425 and 11549). For subsequent  
556 intracellular cytokine analysis, cells were incubated for 6 hs in the presence of anti-  
557 CD28+CD49d antibodies (clones L293 and L25, respectively; both at 1 µg/mL; BD  
558 Biosciences), an anti-CD107a FITC antibody (BD Biosciences), plus brefeldin A (at 10 µg/mL)  
559 and monensin (at 1 µg/mL; BD Biosciences), the two latter added 30 min after the start of all  
560 incubations. In some experiments, cells were culture in RPMI medium without glucose (MP  
561 Biomedicals). CD8<sup>+</sup> T cell proliferation was evaluated by CFSE dilution (at 1 µM, Thermo  
562 Fisher Scientific). In additional experiments, reprogrammed CD8<sup>+</sup> T cells were stimulated with  
563 IL-7 or IL-15 (both at 10 ng/mL; R&D) and cultured for 6 days. In all the cases, cells were  
564 cultured at a density of 2x10<sup>6</sup> cells/mL.

565

566 **Flow cytometry analysis**

567 After cultures, cells were stained with the LIVE/DEAD Fixable Aqua Dead Cell Stain  
568 kit (Thermo Fisher Scientific), with anti-CD3 Alexa Fluor 700 or APC efluor 780 and anti-CD8  
569 PE Texas Red antibodies, accordingly. For phenotype analyses, cells were additionally  
570 stained with anti-CCR7 PE Cy7, anti-CD45RA APC H7, anti-CD27 PerCP Cy5.5, anti-CD95  
571 APC, or anti-CD127 Alexa Fluor 488 antibodies, incubated for 15 minutes at room  
572 temperature. In some experiments, cells were stained with APC-conjugated dextramers  
573 (Immudex), incubated for 10 minutes at room temperature: HLA-A\*0201 (SLYNTVATL) Gag,  
574 HLA-A\*0301 (RLRPGGKKK) Gag, HLA-A\*0301 (QVPLRPMTYK) Nef, and HLA-B\*2705  
575 (KRWIILGLNK) Gag-Pol. Additional surface staining panels included anti-HLA-DR  
576 Superbright 780, anti-CD38 Superbright 600, anti-PD-1 BV421, anti-LAG-3 APC efluor 780,  
577 anti-TIM3 PE Cy7, and anti-TIGIT BV786 antibodies, or anti-CD122 PE and anti-CD215 FITC  
578 antibodies. The BD Transcription Factor Buffer Set kit (BD Biosciences) was used for cell  
579 fixation and permeabilization. Intracellular staining panels for detection of transcription factors  
580 included anti-TCF-1 PE, anti-T-bet V450, anti-Eomes APC, anti-TOX efluor 660, anti-BLIMP1  
581 CF594, or anti-BCL6 Alexa Fluor 488 accordingly. Intracellular cytokine staining panels  
582 included anti-IFN- $\gamma$  PE Cy7 or V450, anti-IL-2 APC-R700, anti-TNF- $\alpha$  PerCP Cy5.5, or anti-  
583 granzyme B Alexa Fluor 647 antibodies, accordingly. In some experiments, cells were fixed  
584 and permeabilized with Phosflow fix/perm buffers (BD Biosciences) and cells were stained  
585 with anti-pS6 Ser235/236 Pacific blue and anti-pAKT Ser473 FITC antibodies (Cell Signaling).  
586 Cell acquisition was performed using LSR II, LSR Fortessa X-20, or ARIA III flow cytometers  
587 (both from BD Biosciences), and data were analyzed with FlowJo v.10 software (BD  
588 Biosciences). The list of flow cytometry antibodies used in this study is shown in  
589 Supplementary Table 4.

590

#### 591 **Measurement of metabolite uptake**

592 CD8<sup>+</sup> T cells were split into four parts and put into contact with 2-NBDG (2-(N-(7-  
593 Nitrobenz-2-oxa-1,3-diazol-4-yl)Amino)-2-Deoxyglucose) (150 μM, 30 min) for glucose  
594 uptake measurement, BODIPY 500/510 C<sub>1</sub>, C<sub>12</sub> (4,4-Difluoro-5-Methyl-4-Bora-3a,4a-Diaza-  
595 s-Indacene-3-Dodecanoic acid) (5 μM, 5 min) for fatty acid uptake measurement, MitoTracker  
596 Green FM (100 nM, 45 min) for mitochondrial mass measurement, and CellROX Deep Red  
597 (5 μM, 30 min) for measurement of oxygen reactive species (all from Thermo Fisher  
598 Scientific). After these incubations, cells were stained with the LIVE/DEAD Fixable Aqua  
599 Dead Cell Stain kit, as well as with phenotype antibodies, as described above.

600

#### 601 **Gene expression analysis in sorted memory cells**

602 Purified CD8<sup>+</sup> T cells were stained with the LIVE/DEAD Fixable Aqua Dead Cell Stain  
603 Kit (Thermo Fisher Scientific) and the following antibodies: anti-CD3 Alexa Fluor 700, anti-  
604 CD8 APC Cy7, anti-CCR7 PE Cy7, anti-CD45RA BV421, and anti-CD27 PE (all from BD  
605 Biosciences). Viable central memory, transitional memory, effector memory, and terminal  
606 effector CD8<sup>+</sup> T cells were bulk sorted (BD FACS ARIA III, BD Biosciences), left rested for at  
607 least 6 hs in complete medium before treatment with the GSK3 inhibitor or vehicle control.  
608 Then, cells were washed and stimulated with plate-bound anti-CD3/CD28 (1 μg/mL) for 48  
609 hs. After culture, cells were counted, and a total of 2,500 cells per condition were put in 96-  
610 well plates containing the VILO Reaction Mix, SUPERase-In, and NP40 (all from Thermo  
611 Fisher Scientific). Plates were snap-frozen and stored at -80°C. Analysis of gene expression  
612 was performed as previously described (8), using Delta Gene primers, 96.96 Dynamic Array  
613 chips, and a Biomark instrument for microfluidics-based qPCR (Fluidigm). Linear derivative  
614 mode baseline correction was applied. Data were normalized using *GAPDH* as a

615 housekeeping gene and using the delta Ct method. Gene expression values are plotted as  
616  $\log 2^{-\Delta Ct}$ .

617

### 618 **Viral suppression assays**

619 PBMC from people with HIV were used to evaluate the capacity of reprogrammed  
620 CD8<sup>+</sup> T cells to suppress HIV infection *ex vivo* (42). CD4<sup>+</sup> and CD8<sup>+</sup> T cells were separated  
621 by, respectively, successive positive and negative magnetic bead sorting (Stemcell  
622 Technologies). Human CD4<sup>+</sup> T cells were cultured for 3 days in complete medium  
623 supplemented with IL-2 (100 IU/mL), in the presence of phytohemagglutinin (PHA; 2 µg/mL).  
624 In parallel, purified CD8<sup>+</sup> T cells were treated with DMSO vehicle control or with the GSK3  
625 inhibitor for 12 hs, followed by washing and incubation for 6 days in complete medium alone.  
626 Then, activated CD4<sup>+</sup> T cells were superinfected with HIV-1 BaL, by spinoculation for 1 h at  
627 2,000 g and 22°C, and cultured alone or with CD8<sup>+</sup> T cells at a 1:1 ratio for 7 days in complete  
628 medium supplemented with IL-2. Viral replication was measured in terms of p24 production  
629 in the culture supernatants using ELISA (XpressBio), or by flow cytometry by quantifying  
630 intracellular HIV-1 Gag products (KC57-FITC antibody [Beckman Coulter]). The HIV-  
631 suppressive capacity of CD8<sup>+</sup> T cells was calculated as the log<sub>10</sub> fold decrease in the median  
632 levels of p24 when CD4<sup>+</sup> T cells were incubated in the presence of CD8<sup>+</sup> T cells. For the  
633 detection of HIV-specific CD8<sup>+</sup> T cells, at the end of the coculture and previous collection of  
634 supernatants, cells were incubated with brefeldin A (10 µg/mL), monensin (2 µg/mL), and an  
635 anti-CD107a BV786 antibody (BD Biosciences), followed by intracellular cytokine staining, as  
636 described above.

637

### 638 **Statistical analyses**

639 GraphPad Prism software version 9.0 was used for statistical analysis. Data are  
640 presented as medians and ranges. The Wilcoxon test was used for the comparison of two  
641 paired data. The Friedman test, and the Dunn's multiple comparisons test, were used for the  
642 comparison of three or more paired groups. The Šidák method was applied to correct for  
643 multiple comparisons, where needed. All P values less than 0.05 were considered as  
644 significant. To determine differentially expressed genes for each CD8<sup>+</sup> T cell memory  
645 population, we defined a mixed effect model including treatment (vehicle control versus GSK3  
646 inhibitor), condition (unstimulated or anti-CD3/CD28 stimulated), and their interaction as fixed  
647 effects, as well as considered participant and technical replicates as a random effect. The  
648 parameters have been estimated using the lme4 package (v1.1-23) in R.

649

#### 650 **Study approval**

651 The study was approved by the ethics committee (Comité de Protection des  
652 Personnes) of Île-de-France XI. All participants gave their informed consent.

653

#### 654 **AUTHOR CONTRIBUTIONS**

655 FP-C and AS-C conceived the study. FP-C, CP, and VM performed experiments and  
656 analyzed the data. SV assisted computational analyses. FB, PT, MM, KB, LW, CJ, CB, CG,  
657 LM, and OL participated in participants recruitment. FP-C and AS-C wrote the manuscript. All  
658 authors revised the manuscript. AS-C provided financial support and supervised the work.

659

#### 660 **ACKNOWLEDGEMENTS**

661 We thank all blood donors from the Établissement Français du Sang (EFS), as well as  
662 the investigators, clinical personal and people with HIV-1 participating to the ANRS EP36 XII  
663 study, ANRS CO6 PRIMO and ANRS CO21 CODEX cohorts for their cooperation. The

664 authors thank Rezak Mahrez and Azeb Tadesse for their help with inclusion of participants.  
665 The authors thank the Cytometry and Biomarkers UTechS platform at Institut Pasteur for  
666 technical support and members of ANRS RHIVIERA consortium for helpful discussion. This  
667 work was funded by ANRS, and NIH UM1AI164562, co-funded by National Heart, Lung and  
668 Blood Institute, National Institute of Diabetes and Digestive and Kidney Diseases, National  
669 Institute of Neurological Disorders and Stroke, National Institute on Drug Abuse and the  
670 National Institute of Allergy and Infectious Diseases. FP-C was supported by ANRS and a  
671 Pasteur-Roux-Cantarini fellowship from Institut Pasteur. The authors thank Gilead for their  
672 support for the acquisition of Fortessa cytometer.

673

#### 674 **DECLARATION OF INTERESTS**

675 Some authors have potential conflict of interest to declare: FP-C, CP, MM-T and AS-  
676 C are listed as inventors in a patent application by Institut Pasteur, partially based on the  
677 results presented here.

678

#### 679 **DATA AND MATERIALS AVAILABILITY**

680 All data and methods reported in this paper are included in the manuscript or in the  
681 supplemental information.

682

683

684

685

686



687 **REFERENCES**

- 688 1. Prlic M, Williams MA, Bevan MJ. Requirements for CD8 T-cell priming, memory generation  
689 and maintenance. [Internet]. *Curr. Opin. Immunol.* 2007;19(3):315–319.
- 690 2. Sáez-Cirión A, Pancino G. HIV controllers: a genetically determined or inducible  
691 phenotype? [Internet]. *Immunol. Rev.* 2013;254(1):281–294.
- 692 3. Collins DR, Gaiha GD, Walker BD. CD8+ T cells in HIV control, cure and prevention  
693 [Internet]. *Nat. Rev. Immunol.* [published online ahead of print: 2020]; doi:10.1038/s41577-  
694 020-0274-9
- 695 4. Migueles SA et al. HIV-specific CD8+ T cell proliferation is coupled to perforin expression  
696 and is maintained in nonprogressors. [Internet]. *Nat. Immunol.* 2002;3(11):1061–1068.
- 697 5. Yan J et al. HIV-Specific CD8+ T Cells from Elite Controllers Are Primed for Survival  
698 [Internet]. *J. Virol.* 2013;87(9):5170–5181.
- 699 6. Betts MR et al. HIV nonprogressors preferentially maintain highly functional HIV-specific  
700 CD8+ T cells [Internet]. *Blood* 2006;107(12):4781–4789.
- 701 7. Rutishauser RL et al. TCF-1 regulates HIV-specific CD8+ T cell expansion capacity.  
702 [Internet]. *JCI insight* 2021;6(3):1–16.
- 703 8. Angin M et al. Metabolic plasticity of HIV-specific CD8+ T cells is associated with enhanced  
704 antiviral potential and natural control of HIV-1 infection [Internet]. *Nat. Metab.* 2019;1:704–  
705 716.
- 706 9. Passaes C et al. Optimal Maturation of the SIV-Specific CD8+ T Cell Response after  
707 Primary Infection Is Associated with Natural Control of SIV: ANRS SIC Study. [Internet]. *Cell*  
708 *Rep.* 2020;32(12):108174.
- 709 10. Saez-Cirion A et al. HIV controllers exhibit potent CD8 T cell capacity to suppress HIV  
710 infection ex vivo and peculiar cytotoxic T lymphocyte activation phenotype [Internet]. *Proc.*  
711 *Natl. Acad. Sci.* 2007;104(16):6776–6781.

- 712 11. Escobar G, Mangani D, Anderson AC. T cell factor 1: A master regulator of the T cell  
713 response in disease. [Internet]. *Sci. Immunol.* 2020;5(53):1–12.
- 714 12. Gattinoni L, Klebanoff CA, Restifo NP. Paths to stemness: building the ultimate antitumour  
715 T cell. [Internet]. *Nat. Rev. Cancer* 2012;12(10):671–684.
- 716 13. Utzschneider DT et al. T Cell Factor 1-Expressing Memory-like CD8+ T Cells Sustain the  
717 Immune Response to Chronic Viral Infections. [Internet]. *Immunity* 2016;45(2):415–427.
- 718 14. Wu T et al. The TCF1-Bcl6 axis counteracts type I interferon to repress exhaustion and  
719 maintain T cell stemness. [Internet]. *Sci. Immunol.* 2016;1(6):1–12.
- 720 15. Wieland D et al. TCF1+ hepatitis C virus-specific CD8+ T cells are maintained after  
721 cessation of chronic antigen stimulation. [Internet]. *Nat. Commun.* 2017;8:1–13.
- 722 16. Sekine T et al. TOX is expressed by exhausted and polyfunctional human effector memory  
723 CD8+ T cells [Internet]. *Sci. Immunol.* 2020;5(49):eaba7918.
- 724 17. Kishton RJ, Sukumar M, Restifo NP. Metabolic Regulation of T Cell Longevity and  
725 Function in Tumor Immunotherapy. [Internet]. *Cell Metab.* 2017;26(1):94–109.
- 726 18. Pollizzi KN et al. mTORC1 and mTORC2 selectively regulate CD8+ T cell differentiation  
727 [Internet]. *J. Clin. Invest.* 2015;125(5):2090–2108.
- 728 19. Araki K et al. mTOR regulates memory CD8 T-cell differentiation. [Internet]. *Nature*  
729 2009;460(7251):108–112.
- 730 20. Scholz G et al. Modulation of mTOR Signalling Triggers the Formation of Stem Cell-like  
731 Memory T Cells [Internet]. *EBioMedicine* 2016;4:50–61.
- 732 21. Gattinoni L et al. Wnt signaling arrests effector T cell differentiation and generates CD8+  
733 memory stem cells. [Internet]. *Nat. Med.* 2009;15(7):808–813.
- 734 22. Kaech SM, Cui W. Transcriptional control of effector and memory CD8+ T cell  
735 differentiation [Internet]. *Nat. Rev. Immunol.* 2012;12(11):749–761.
- 736 23. Liu Z et al. Cutting Edge: Transcription Factor BCL6 Is Required for the Generation, but

737 Not Maintenance, of Memory CD8+ T Cells in Acute Viral Infection [Internet]. *J. Immunol.*  
738 2019;203:ji1900014.

739 24. Zhou X et al. Differentiation and persistence of memory CD8+ T cells depend on T cell  
740 factor 1. [Internet]. *Immunity* 2010;33(2):229–240.

741 25. Schluns KS, Kieper WC, Jameson SC, Lefrançois L. Interleukin-7 mediates the  
742 homeostasis of naïve and memory CD8 T cells in vivo. [Internet]. *Nat. Immunol.*  
743 2000;1(5):426–432.

744 26. Khan O et al. TOX transcriptionally and epigenetically programs CD8+ T cell exhaustion  
745 [Internet]. *Nature* 2019;571(7764):211–218.

746 27. Yao C et al. Single-cell RNA-seq reveals TOX as a key regulator of CD8+ T cell  
747 persistence in chronic infection [Internet]. *Nat. Immunol.* 2019;20(7):890–901.

748 28. Page N et al. Expression of the DNA-Binding Factor TOX Promotes the Encephalitogenic  
749 Potential of Microbe-Induced Autoreactive CD8+ T Cells [Internet]. *Immunity* 2018;48(5):937-  
750 950.e8.

751 29. Verma NK, Kelleher D. Not Just an Adhesion Molecule: LFA-1 Contact Tunes the T  
752 Lymphocyte Program. [Internet]. *J. Immunol.* 2017;199(4):1213–1221.

753 30. Kurachi M et al. The transcription factor BATF operates as an essential differentiation  
754 checkpoint in early effector CD8+ T cells [Internet]. *Nat. Immunol.* 2014;15(4):373–383.

755 31. Sercan Ö, Stoycheva D, Hämmerling GJ, Arnold B, Schüler T. IFN- $\gamma$  Receptor Signaling  
756 Regulates Memory CD8+ T Cell Differentiation [Internet]. *J. Immunol.* 2010;184(6):2855 LP  
757 – 2862.

758 32. McLane LM, Abdel-Hakeem MS, Wherry EJ. CD8 T Cell Exhaustion During Chronic Viral  
759 Infection and Cancer. [Internet]. *Annu. Rev. Immunol.* 2019;37:457–495.

760 33. Chapman NM, Boothby MR, Chi H. Metabolic coordination of T cell quiescence and  
761 activation [Internet]. *Nat. Rev. Immunol.* 2020;20(1):55–70.

- 762 34. Salmond RJ. mTOR Regulation of Glycolytic Metabolism in T Cells [Internet]. *Front. Cell*  
763 *Dev. Biol.* 2018;6:122.
- 764 35. Michalek RD et al. Estrogen-related receptor- $\alpha$  is a metabolic regulator of effector T-cell  
765 activation and differentiation [Internet]. *Proc. Natl. Acad. Sci. U. S. A.* 2011;108(45):18348–  
766 18353.
- 767 36. Johnson MO et al. Distinct Regulation of Th17 and Th1 Cell Differentiation by  
768 Glutaminase-Dependent Metabolism [Internet]. *Cell* 2018;175(7):1780-1795.e19.
- 769 37. Rao E et al. Deficiency of AMPK in CD8<sup>+</sup> T cells suppresses their anti-tumor function by  
770 inducing protein phosphatase-mediated cell death [Internet]. *Oncotarget* 2015;6(10):7944–  
771 7958.
- 772 38. Reina-Campos M, Scharping NE, Goldrath AW. CD8<sup>+</sup> T cell metabolism in infection and  
773 cancer [Internet]. *Nat. Rev. Immunol.* 2021;21(11):718–738.
- 774 39. Chowdhury FZ et al. Metabolic pathway activation distinguishes transcriptional signatures  
775 of CD8<sup>+</sup> T cells from HIV-1 elite controllers. [Internet]. *AIDS* 2018;32(18):2669–2677.
- 776 40. Powell JD, Pollizzi KN, Heikamp EB, Horton MR. Regulation of immune responses by  
777 mTOR. [Internet]. *Annu. Rev. Immunol.* 2012;30:39–68.
- 778 41. Jagannathan P et al. Comparisons of CD8<sup>+</sup> T cells specific for human immunodeficiency  
779 virus, hepatitis C virus, and cytomegalovirus reveal differences in frequency,  
780 immunodominance, phenotype, and interleukin-2 responsiveness. [Internet]. *J. Virol.*  
781 2009;83(6):2728–2742.
- 782 42. Sáez-Cirión A, Shin SY, Versmisse P, Barré-Sinoussi F, Pancino G. Ex vivo T cell-based  
783 HIV suppression assay to evaluate HIV-specific CD8<sup>+</sup> T-cell responses. [Internet]. *Nat.*  
784 *Protoc.* 2010;5(6):1033–1041.
- 785 43. Sáez-Cirión A et al. Heterogeneity in HIV suppression by CD8 T cells from HIV controllers:  
786 association with Gag-specific CD8 T cell responses. [Internet]. *J. Immunol.*

787 2009;182(12):7828–7837.

788 44. Boyman O, Purton JF, Surh CD, Sprent J. Cytokines and T-cell homeostasis. [Internet].  
789 *Curr. Opin. Immunol.* 2007;19(3):320–326.

790 45. Meijer L et al. GSK-3-selective inhibitors derived from Tyrian purple indirubins. [Internet].  
791 *Chem. Biol.* 2003;10(12):1255–1266.

792 46. Shan Q et al. Ectopic Tcf1 expression instills a stem-like program in exhausted CD8+ T  
793 cells to enhance viral and tumor immunity [Internet]. *Cell. Mol. Immunol.* 2021;18(5):1262–  
794 1277.

795 47. Im SJ et al. Defining CD8+ T cells that provide the proliferative burst after PD-1 therapy  
796 [Internet]. *Nature* 2016;537:417–421.

797 48. Miller BC et al. Subsets of exhausted CD8+ T cells differentially mediate tumor control  
798 and respond to checkpoint blockade [Internet]. *Nat. Immunol.* 2019;20(3):326–336.

799 49. Galletti G et al. Two subsets of stem-like CD8+ memory T cell progenitors with distinct  
800 fate commitments in humans. [Internet]. *Nat. Immunol.* 2020;21(12):1552–1562.

801 50. Hermida MA, Dinesh Kumar J, Leslie NR. GSK3 and its interactions with the  
802 PI3K/AKT/mTOR signalling network [Internet]. *Adv. Biol. Regul.* 2017;65:5–15.

803 51. Koo J, Wu X, Mao Z, Khuri FR, Sun S-Y. Rictor Undergoes Glycogen Synthase Kinase 3  
804 (GSK3)-dependent, FBXW7-mediated Ubiquitination and Proteasomal Degradation\*  
805 [Internet]. *J. Biol. Chem.* 2015;290(22):14120–14129.

806 52. Huang H, Long L, Zhou P, Chapman NM, Chi H. mTOR signaling at the crossroads of  
807 environmental signals and T-cell fate decisions [Internet]. *Immunol. Rev.* 2020;295(1):15–38.

808 53. Johnnidis JB et al. Inhibitory signaling sustains a distinct early memory CD8+ T cell  
809 precursor that is resistant to DNA damage [Internet]. *Sci. Immunol.* 2021;6(55):eabe3702.

810 54. Lin W-HW et al. CD8+ T Lymphocyte Self-Renewal during Effector Cell Determination.  
811 [Internet]. *Cell Rep.* 2016;17(7):1773–1782.

- 812 55. Zhang L, Romero P. Metabolic Control of CD8+ T Cell Fate Decisions and Antitumor  
813 Immunity. [Internet]. *Trends Mol. Med.* 2018;24(1):30–48.
- 814 56. Pearce EL et al. Enhancing CD8 T-cell memory by modulating fatty acid metabolism  
815 [Internet]. *Nature* 2009;460(7251):103–107.
- 816 57. Sukumar M et al. Inhibiting glycolytic metabolism enhances CD8+ T cell memory and  
817 antitumor function [Internet]. *J. Clin. Invest.* 2013;123(10):4479–4488.
- 818 58. Crompton JG et al. Lineage relationship of CD8+ T cell subsets is revealed by progressive  
819 changes in the epigenetic landscape [Internet]. *Cell. Mol. Immunol.* 2016;13(4):502–513.
- 820 59. Valle-Casuso JC et al. Cellular Metabolism Is a Major Determinant of HIV-1 Reservoir  
821 Seeding in CD4(+) T Cells and Offers an Opportunity to Tackle Infection. [Internet]. *Cell*  
822 *Metab.* 2019;29(3):611-626.e5.
- 823 60. Lim AR, Rathmell WK, Rathmell JC. The tumor microenvironment as a metabolic barrier  
824 to effector T cells and immunotherapy [Internet]. *Elife* 2020;9:e55185.
- 825 61. Day CL et al. PD-1 expression on HIV-specific T cells is associated with T-cell exhaustion  
826 and disease progression [Internet]. *Nature* 2006;443(7109):350–4.
- 827 62. Trautmann L et al. Upregulation of PD-1 expression on HIV-specific CD8+ T cells leads  
828 to reversible immune dysfunction [Internet]. *Nat. Med.* 2006;12(10):1198–1202.
- 829 63. Brehm MA, Daniels KA, Welsh RM. Rapid production of TNF-alpha following TCR  
830 engagement of naive CD8 T cells. [Internet]. *J. Immunol.* 2005;175(8):5043–5049.
- 831 64. Denton AE, Russ BE, Doherty PC, Rao S, Turner SJ. Differentiation-dependent functional  
832 and epigenetic landscapes for cytokine genes in virus-specific CD8+ T cells. [Internet]. *Proc.*  
833 *Natl. Acad. Sci. U. S. A.* 2011;108(37):15306–15311.
- 834 65. Yao C et al. BACH2 enforces the transcriptional and epigenetic programs of stem-like  
835 CD8+ T cells [Internet]. *Nat. Immunol.* 2021;22(3):370–380.
- 836 66. Salerno F, Paolini NA, Stark R, von Lindern M, Wolkers MC. Distinct PKC-mediated

837 posttranscriptional events set cytokine production kinetics in CD8+ T cells [Internet]. *Proc.*  
838 *Natl. Acad. Sci.* 2017;114(36):9677 LP – 9682.

839 67. Lane BR et al. TNF- $\alpha$  Inhibits HIV-1 Replication in Peripheral Blood Monocytes and  
840 Alveolar Macrophages by Inducing the Production of RANTES and Decreasing C-C  
841 Chemokine Receptor 5 (CCR5) Expression [Internet]. *J. Immunol.* 1999;163(7):3653 LP –  
842 3661.

843 68. Herbein G, Montaner LJ, Gordon S. Tumor necrosis factor alpha inhibits entry of human  
844 immunodeficiency virus type 1 into primary human macrophages: a selective role for the 75-  
845 kilodalton receptor.. *J. Virol.* 1996;70(11):7388–7397.

846 69. Foley MH et al. High avidity CD8+ T cells efficiently eliminate motile HIV-infected targets  
847 and execute a locally focused program of anti-viral function [Internet]. *PLoS One*  
848 2014;9(2):e87873–e87873.

849 70. Lichterfeld M et al. HIV-1–specific cytotoxicity is preferentially mediated by a subset of  
850 CD8+ T cells producing both interferon- $\gamma$  and tumor necrosis factor- $\alpha$  [Internet]. *Blood*  
851 2004;104(2):487–494.

852 71. Duh EJ, Maury WJ, Folks TM, Fauci AS, Rabson AB. Tumor necrosis factor alpha  
853 activates human immunodeficiency virus type 1 through induction of nuclear factor binding  
854 to the NF-kappa B sites in the long terminal repeat.. *Proc. Natl. Acad. Sci. U. S. A.*  
855 1989;86(15):5974–5978.

856 72. Quivy V et al. Synergistic activation of human immunodeficiency virus type 1 promoter  
857 activity by NF-kappaB and inhibitors of deacetylases: potential perspectives for the  
858 development of therapeutic strategies. [Internet]. *J. Virol.* 2002;76(21):11091–11103.

859 73. Lieberman J et al. Safety of autologous, ex vivo-expanded human immunodeficiency virus  
860 (HIV)-specific cytotoxic T-lymphocyte infusion in HIV-infected patients. [Internet]. *Blood*  
861 1997;90(6):2196–2206.

862 74. Tan R et al. Rapid death of adoptively transferred T cells in acquired immunodeficiency  
863 syndrome. [Internet]. *Blood* 1999;93(5):1506–1510.

864 75. Brodie SJ et al. In vivo migration and function of transferred HIV-1-specific cytotoxic T  
865 cells. [Internet]. *Nat. Med.* 1999;5(1):34–41.

866 76. Krishna S et al. Stem-like CD8 T cells mediate response of adoptive cell immunotherapy  
867 against human cancer [Internet]. *Science (80-. )*. 2020;370(6522):1328 LP – 1334.

868 77. Deng K et al. Broad CTL response is required to clear latent HIV-1 due to dominance of  
869 escape mutations. [Internet]. *Nature* 2015;517(7534):381–385.

870 78. Augello G et al. The Role of GSK-3 in Cancer Immunotherapy: GSK-3 Inhibitors as a New  
871 Frontier in Cancer Treatment [Internet]. *Cells* 2020;9(6):1427.

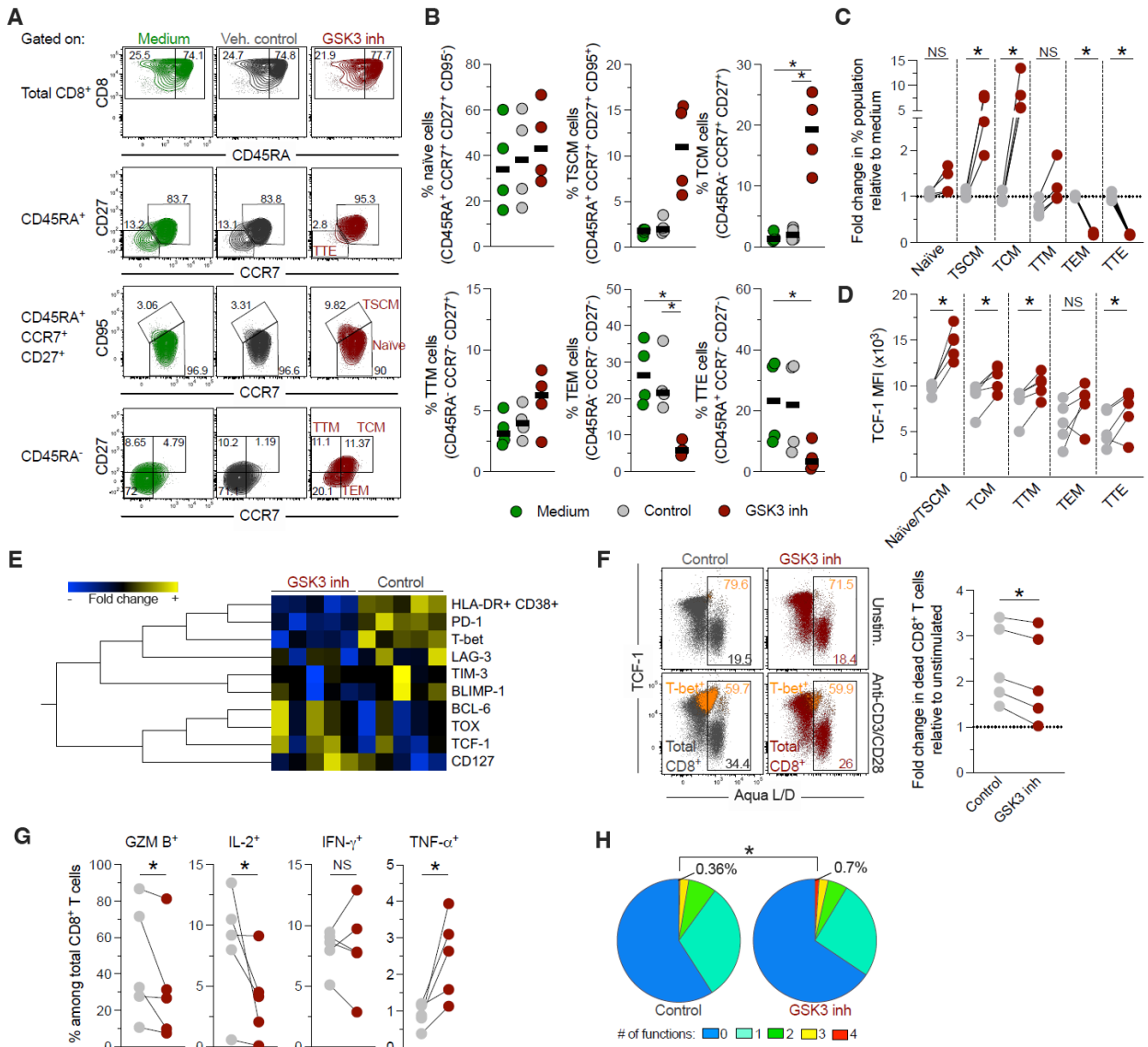
872 79. Arciniegas Ruiz SM, Eldar-Finkelman H. Glycogen Synthase Kinase-3 Inhibitors:  
873 Preclinical and Clinical Focus on CNS-A Decade Onward.. *Front. Mol. Neurosci.*  
874 2021;14:792364.

875

876



877 **FIGURES**



878

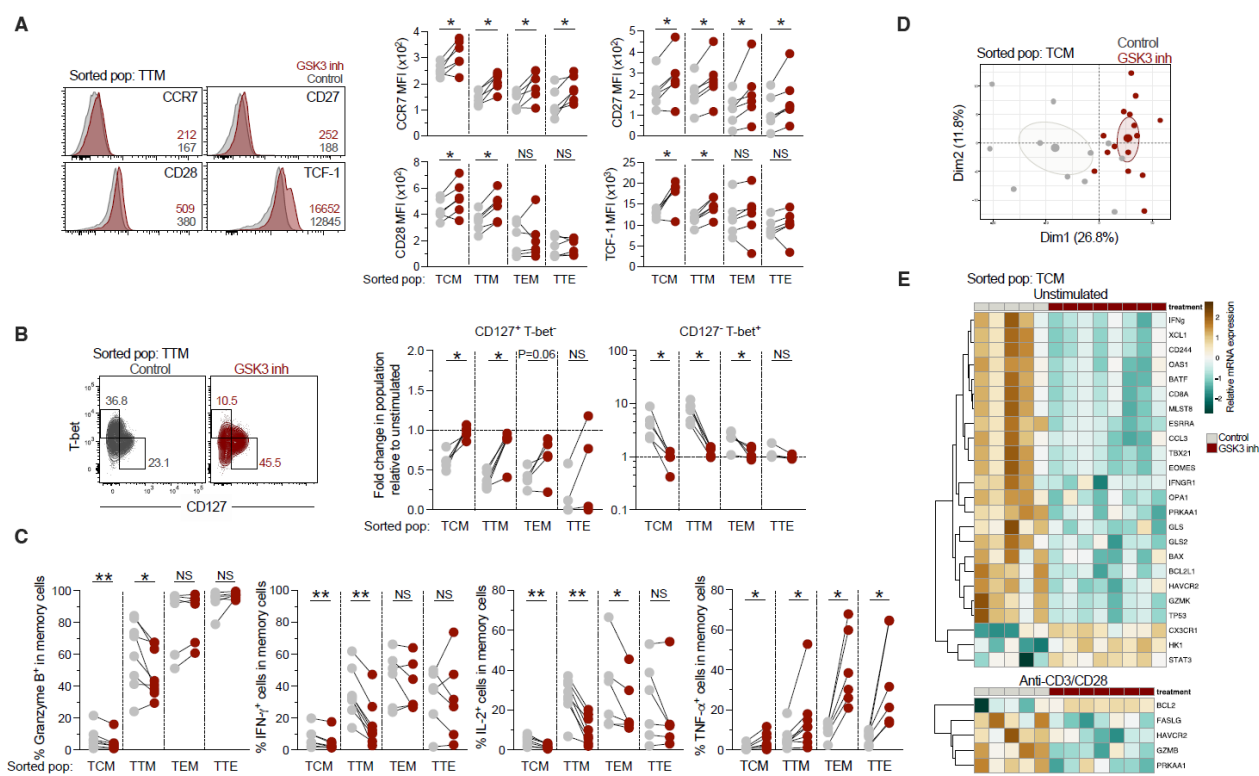
879

880 **Figure 1. Induction of stem-like CD8<sup>+</sup> T cells with high survival capacity and**  
 881 **polyfunctionality by in vitro reprogramming.** Total CD8<sup>+</sup> T cells from people without HIV  
 882 were treated with medium, vehicle control, or the GSK3 inhibitor, followed by incubation under  
 883 basal conditions or anti-CD3/CD28 stimulation for 48 hs. **A-B.** Analysis of CD8<sup>+</sup> T cell  
 884 subpopulations in unstimulated cells (n=4; Dunn's test). **C.** Fold change of CD8<sup>+</sup> T cell  
 885 subpopulations upon vehicle control or a GSK3 inhibitor treatment, relative to medium alone

886 condition (n=4). **D.** Expression of TCF-1 in CD8<sup>+</sup> T cell subsets (n=4). **E.** Fold change in the  
887 expression of the indicated markers induced by anti-CD3/CD28 stimulation, relative to  
888 unstimulated cells (n=5). **F.** Analysis of dead cells (Aqua Live/Dead<sup>+</sup>) among total and T-bet<sup>+</sup>  
889 CD8<sup>+</sup> T cells, and fold change in dead CD8<sup>+</sup> T cells induced by anti-CD3/CD28 stimulation,  
890 relative to the unstimulated condition (n=5). **G.** Frequencies of granzyme B<sup>+</sup>, IL-2<sup>+</sup>, IFN- $\gamma$ <sup>+</sup>,  
891 and TNF- $\alpha$ <sup>+</sup> CD8<sup>+</sup> T cells after anti-CD3/CD28 stimulation. **H.** Expression of 1 to 4 functions  
892 in CD8<sup>+</sup> T cells (n=5). \* $P < 0.05$ ; \*\* $P \leq 0.01$ . NS: Not statistically significant. In C-D, and F-H,  
893 the Wilcoxon test was used. The data obtained in two (A-F) or three (G,H) independent  
894 experiments is shown.

895

896



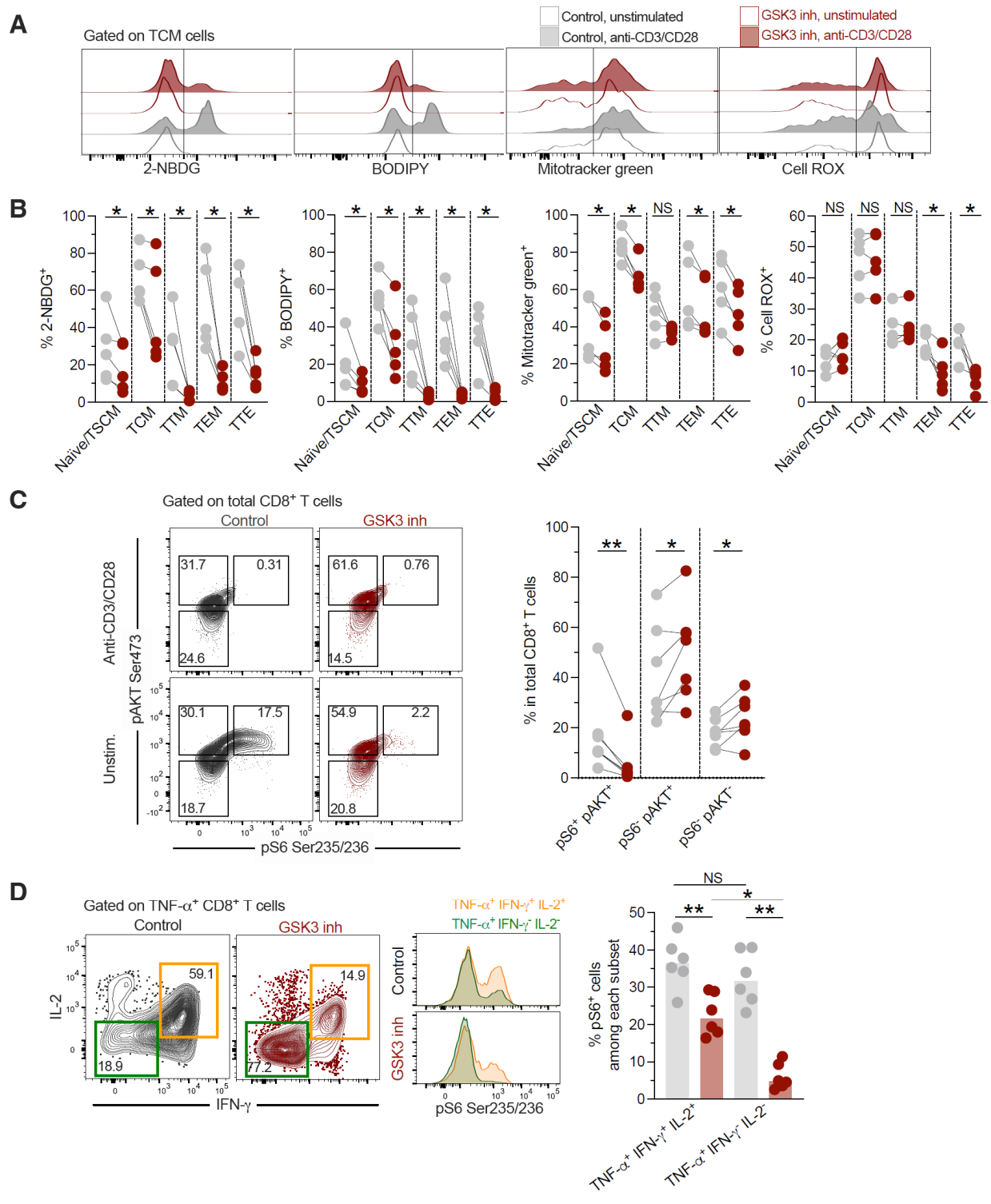
897

898 **Figure 2. Intrinsic effects of reprogramming in CD8<sup>+</sup> T cell memory subpopulations.**

899 Sorted TCM, TTM, TEM and TEM from people without HIV were treated with the GSK3  
900 inhibitor or vehicle control, followed by incubation under basal conditions or anti-CD3/CD28  
901 stimulation for 48 hs. **A.** Representative histograms showing the expression of CCR7, CD27,  
902 CD28, and TCF-1 in sorted TTM cells, in basal conditions. The median fluorescence intensity  
903 of each marker is depicted. The summary of the expression of each marker in memory cells  
904 after vehicle control or GSK3 inhibitor treatment, in the absence of stimulation, is shown. **B.**  
905 Flow cytometry analysis of CD127<sup>+</sup> T-bet<sup>-</sup> and CD127<sup>-</sup> T-bet<sup>+</sup> cells after anti-CD3/CD28  
906 stimulation, and fold change in the indicated subsets among memory cells induced by anti-  
907 CD3/CD28 stimulation, relative to the unstimulated condition. **C.** Frequencies of granzyme  
908 B<sup>+</sup>, IFN- $\gamma$ <sup>+</sup>, IL-2<sup>+</sup>, and TNF- $\alpha$ <sup>+</sup> among memory cells after anti-CD3/CD28 stimulation. At least  
909 5 donors were included for each comparison; data from 7 independent experiments. \* $P < 0.05$ ;  
910 \*\* $P \leq 0.01$ ; NS: Not statistically significant; Wilcoxon test. **D.** Principal Component Analysis

911 (PCA) of gene expression by TCM cells treated with vehicle control or GSK3 inhibitor. **E.** Heat  
912 map of genes differentially expressed ( $P < 0.05$  according to a mixed effect model) in  
913 reprogrammed versus non-reprogrammed TCM cells. The scale on the heatmap indicates  
914 the mRNA levels relative to the housekeeping gene (*GAPDH*) and plotted as  $\log 2^{-\Delta C_t}$ , in  
915 unstimulated and polyclonally-stimulated cells (At least 5 donors were included for each  
916 comparison; data from two independent experiments).

917



918

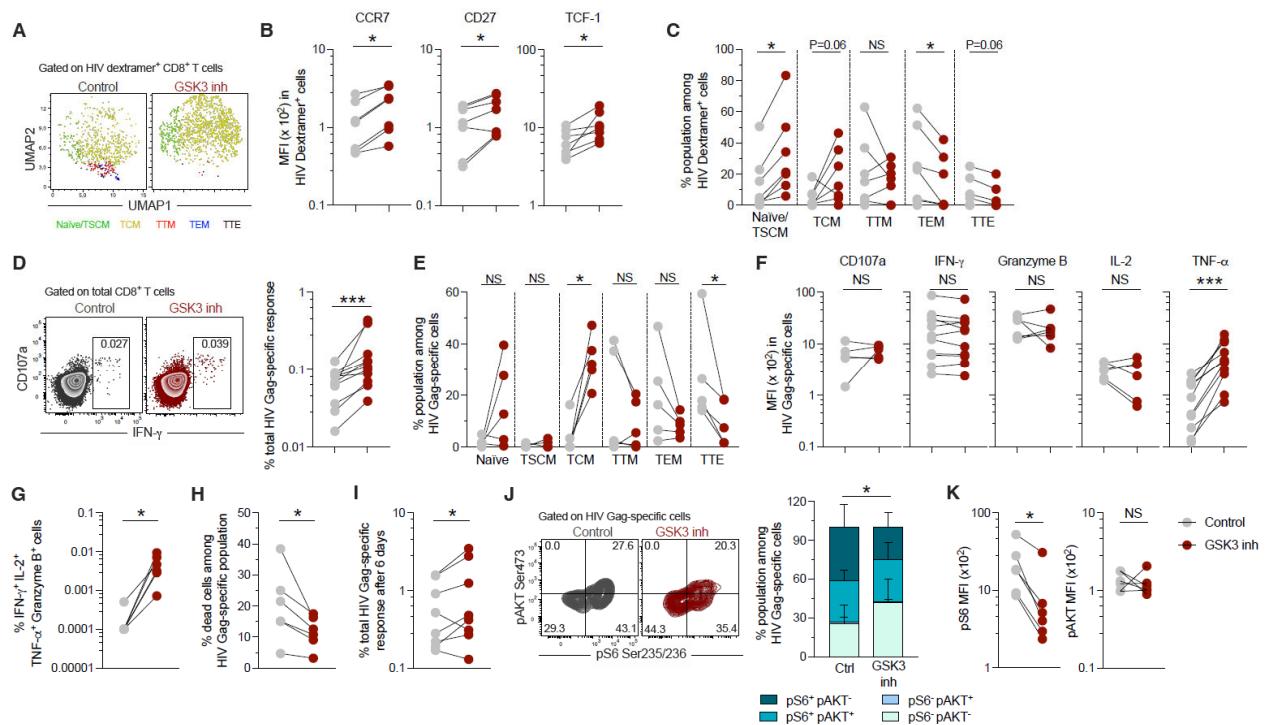
919 **Figure 3. Modulation of anabolic metabolism in reprogrammed CD8<sup>+</sup> T cells.** A-B. Total

920 CD8<sup>+</sup> T cells from people without HIV were treated with vehicle control or the GSK3 inhibitor,

921 followed by incubation under basal conditions or anti-CD3/CD28 stimulation for 48 hs. Then,

922 the expression of 2-NBDG, BODIPY, Mitotracker green, and Cell ROX among CD8<sup>+</sup> T cell  
923 subsets was evaluated (**A**). In **B**, the frequencies of 2-NBDG<sup>+</sup>, BODIPY<sup>+</sup>, Mitotracker green<sup>+</sup>,  
924 and Cell ROX<sup>+</sup> in CD8<sup>+</sup> T cell subpopulations after stimulation are shown (n=5; Wilcoxon test).  
925 **C-D**. Total CD8<sup>+</sup> T cells from people without HIV were treated with vehicle control or the GSK3  
926 inhibitor, followed by incubation under basal conditions or anti-CD3/CD28 stimulation for 48  
927 hs. **C**. Flow cytometry analysis of the expression of pS6 and pAKT in total CD8<sup>+</sup> T cells, and  
928 frequencies of pS6<sup>+</sup> pAKT<sup>+</sup>, pS6<sup>-</sup> pAKT<sup>+</sup> and pS6<sup>-</sup> pAKT<sup>-</sup> subsets in total CD8<sup>+</sup> T cells (n=7;  
929 Wilcoxon test). **D**. Flow cytometry analysis of the expression of IL-2 and IFN- $\gamma$  among TNF-  
930  $\alpha$ <sup>+</sup> CD8<sup>+</sup> T cells, after anti-CD3/CD28 stimulation. The histograms show the expression of  
931 pS6 in the indicated subsets, in reprogrammed and non-reprogrammed cells. The frequency  
932 of pS6<sup>+</sup> cells among TNF- $\alpha$ <sup>+</sup> IFN- $\gamma$ <sup>+</sup> IL-2<sup>+</sup> or TNF- $\alpha$ <sup>+</sup> IFN- $\gamma$ <sup>-</sup> IL-2<sup>-</sup> subsets is shown (n=6 people  
933 without HIV; Šidák multiple comparison test). \* $P < 0.05$ ; \*\* $P \leq 0.01$ ; NS: Not statistically  
934 significant. Data were obtained in two independent experiments.

935



936

937

938

939

940

941

942

943

944

945

946

947

948

949

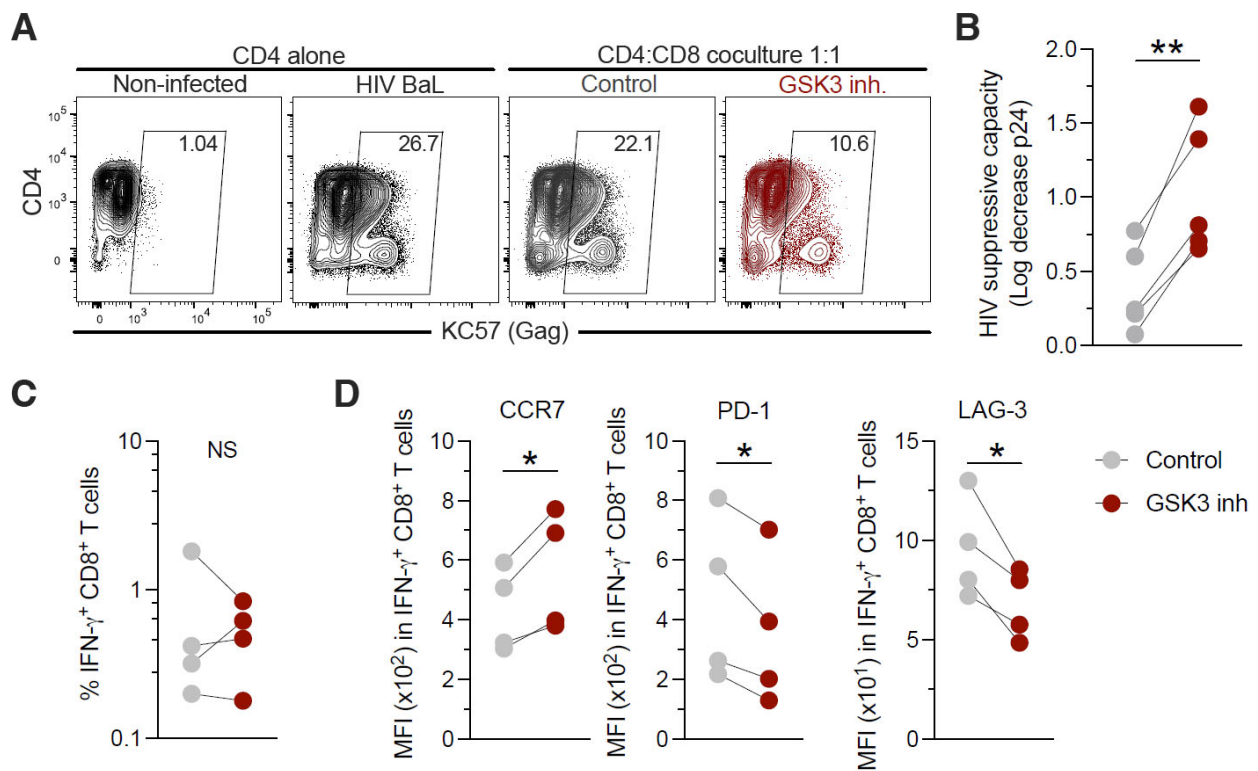
950

**Figure 4. Enhanced functionality and survival of reprogrammed HIV-specific CD8<sup>+</sup> T cells.** After treatment with the GSK3 inhibitor, CD8<sup>+</sup> T cells from people with HIV were stained with HLA-matched HIV dextramers, for the analysis of the phenotype of HIV dextramer<sup>+</sup> cells **A**. UMAP plots generated from HIV dextramer<sup>+</sup> CD8<sup>+</sup> T cells after data concatenation (n=4). Vehicle control and GSK3 inhibitor treatments, as well as CD8<sup>+</sup> T cell subpopulations were identified by manual gating and projected into the UMAP space. **B**. Summary of the expression of CCR7, CD27 and TCF-1 in HIV dextramer<sup>+</sup> CD8<sup>+</sup> T cells (n=7). **C**. Frequencies of CD8<sup>+</sup> T cell subpopulations among HIV dextramer<sup>+</sup> CD8<sup>+</sup> T cells (n=7). **D-G**. After reprogramming, cells from people with HIV were stimulated for 6 hs with Gag peptides, for the analysis of the total frequency (IFN- $\gamma$ <sup>+</sup> or CD107a<sup>+</sup> or IL-2<sup>+</sup> or TNF- $\alpha$ <sup>+</sup>) of antigen-specific CD8<sup>+</sup> T cells (n=5) (**D**), the proportion of memory subpopulations (n=5) (**E**), the expression of CD107a, IFN- $\gamma$ , granzyme B, IL-2, and TNF- $\alpha$  on a per cell basis (n=5-11) (**F**), and the frequency of polyfunctional cells (n=6) (**G**). **H-I**. Cells from people with HIV were stimulated for 6 days with Gag peptides and re-stimulated with the same peptides for another 12 hs, for

951 the analysis of the viability of proliferating HIV Gag-specific CD8<sup>+</sup> T cells (n=6) (**H**), and the  
952 frequency of the total (live IFN- $\gamma$ <sup>+</sup> or IL-2<sup>+</sup> or TNF- $\alpha$ <sup>+</sup>) HIV Gag-specific response (n=8) (**I**). **J-**  
953 **K**. After reprogramming, cells from people with HIV (n=6) were stimulated for 6 hs with Gag  
954 peptides, for the analysis of pS6<sup>+</sup> pAKT<sup>-</sup>, pS6<sup>+</sup> pAKT<sup>+</sup>, pS6<sup>-</sup> pAKT<sup>+</sup> and pS6<sup>-</sup> pAKT<sup>-</sup> subsets  
955 (**J**) or the intensity of expression of pS6 and pAKT (**K**) in HIV Gag-specific (IFN- $\gamma$ <sup>+</sup> and/or IL-  
956 2<sup>+</sup>) CD8<sup>+</sup> T cells. \* $P < 0.05$ ; \*\*\* $P \leq 0.001$ ; NS: Not statistically significant; Wilcoxon test. Data  
957 were obtained in three independent experiments.

958



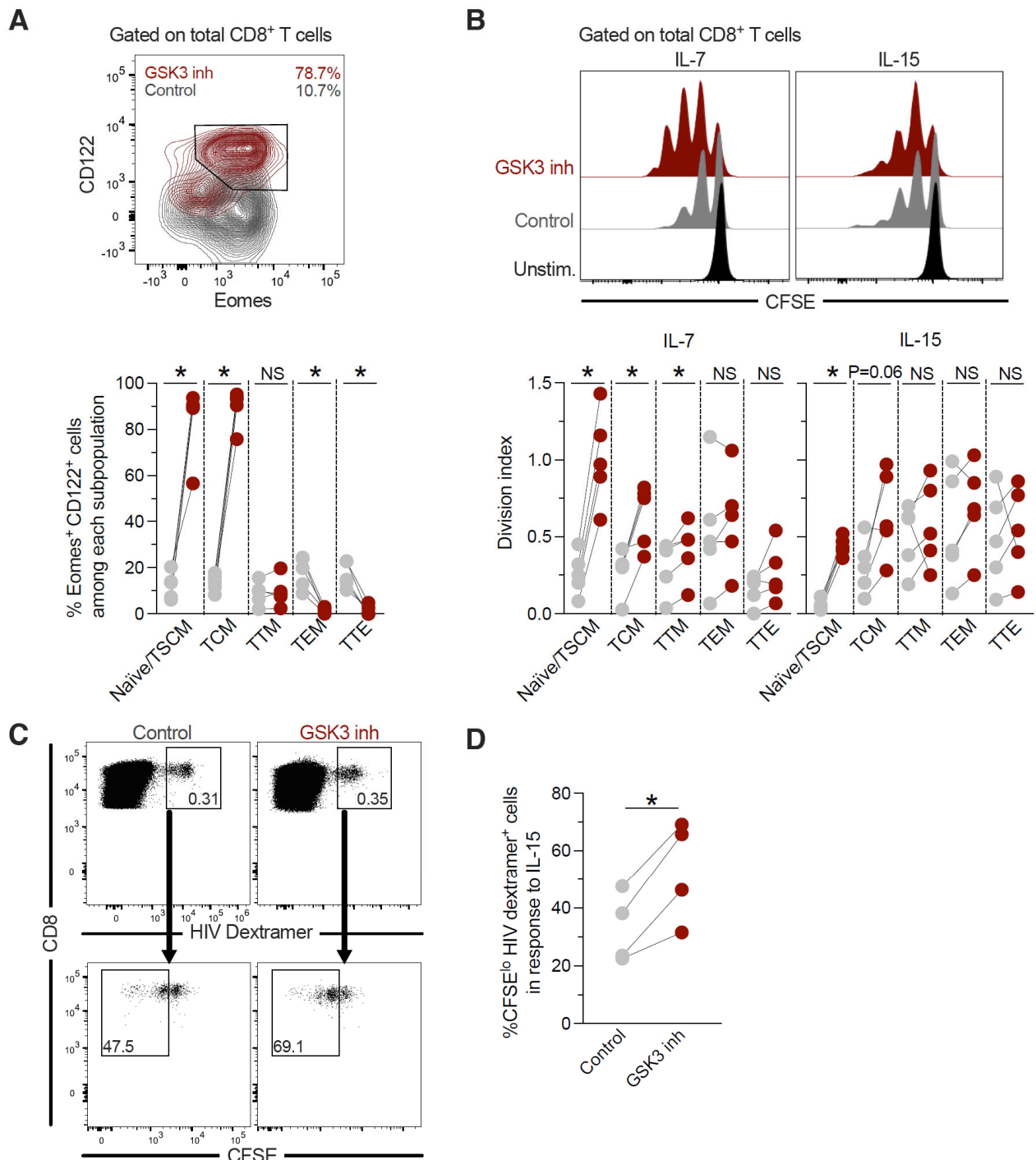


959

960 **Figure 5. Reprogramming increases the HIV-1 suppressive capacity of CD8<sup>+</sup> T cells.**

961 HIV-1 BaL-superinfected CD4<sup>+</sup> T cells from people with HIV were cultured alone or in the  
 962 presence of autologous non-reprogrammed or reprogrammed CD8<sup>+</sup> T cells. After 7 days, the  
 963 levels of infection were measured by flow cytometry (KC57 anti-Gag antibody) or ELISA (p24  
 964 in culture supernatant). **A.** Representative flow cytometry analysis of the frequency of infected  
 965 CD4<sup>+</sup> T cells (from a total of 4 donors). **B.** HIV suppressive capacity of non-reprogrammed  
 966 and reprogrammed CD8<sup>+</sup> T cells (Log<sub>10</sub> decrease of p24 levels in culture supernatant; n=5  
 967 individuals, median of triplicates for each experiment). **C-D** The frequency of IFN- $\gamma$ <sup>+</sup> HIV-  
 968 specific CD8<sup>+</sup> T cells (**C**) and the expression of CCR7, PD-1, and LAG-3 in HIV-specific CD8<sup>+</sup>  
 969 T cells (**D**) were measured after 7 days of coculture. \**P*<0.05; \*\**P*≤0.01; NS: Not statistically  
 970 significant; Wilcoxon test.

971



972

973 **Figure 6. Superior response to  $\gamma$ -chain cytokines by reprogrammed HIV-specific CD8<sup>+</sup>**  
 974 **T cells.** **A.** Total CD8<sup>+</sup> T cells from people without HIV were treated with vehicle control or  
 975 the GSK3 inhibitor, followed by evaluation of the expression of Eomes and CD122 in CD8<sup>+</sup> T  
 976 cell subsets (n=5). **B.** After vehicle control or GSK3 inhibitor treatment, CD8<sup>+</sup> T cells from

977 people without HIV were left unstimulated or stimulated with IL-7 or IL-15 for 6 days, for the  
978 analysis of cell proliferation (n=5, data from two independent experiments). **C-D**. CD8<sup>+</sup> T cells  
979 from people with HIV were treated with vehicle control or the GSK3 inhibitor, followed by  
980 stimulation with IL-15 for 6 days, for the analysis of the proliferation of HIV dextramer<sup>+</sup> CD8<sup>+</sup>  
981 T cells (n=4; data from three independent experiments). \**P*<0.05; NS: Not statistically  
982 significant; Wilcoxon test.